PCoMS OpenMX Hands-on Tutorial

Program:

9:30-10:40	Introduction of DFT and OpenMX
10:40-11:10	Hands-on lecture
11:10-12:00	Login to computer and perform test calculations
12:00-13:00	Lunch
13:00-13:30	Geometry optimization, NEB calculations, and molecular dynamics
13:30-14:10	Practical session (take a break properly)
14:10-14:40	Calculations of X-ray photoemission spectra
14:40-15:20	Practical session (take a break properly)
15:20-15:50	Electronic transport calculations by NEGF
15:50-16:30	Practical session (take a break properly)
16:30-17:00	Discussion session

Taisuke Ozaki (ISSP, Univ. of Tokyo)
Mitsuaki Kawamura (ISSP, Univ. of Tokyo)

Institute for Materials Research (IMR), Tohoku University, Feb. 14, 2020.

Purposes of the tutorial

The first-principles calculations based on density functional theories (DFT) have been playing an indispensable role in deeply understanding physical and chemical properties of materials in recent years.

In the tutorial, we would like to introduce OpenMX based on DFT, optimized numerical basis orbitals, and pseudopotential with practical calculations so that that you can get familiar with OpenMX calculations.

Any questions regarding OpenMX calculations are welcome. We hope that OpenMX can be useful for your future researches.

OpenMX Open source package for Material eXplorer

- Software package for density functional calculations of molecules and bulks
- Norm-conserving pseudopotentials (PPs)
- Variationally optimized numerical atomic basis functions

Basic functionalities

- SCF calc. by LDA, GGA, DFT+U
- Total energy and forces on atoms
- Band dispersion and density of states
- Geometry optimization by BFGS, RF, EF
- Charge analysis by Mullken, Voronoi, ESP
- Molecular dynamics with NEV and NVT ensembles
- Charge doping
- Fermi surface
- Analysis of charge, spin, potentials by cube files
- Database of optimized PPs and basis funcitons

Extensions

- O(N) and low-order scaling diagonalization
- Non-collinear DFT for non-collinear magnetism
- Spin-orbit coupling included self-consistently
- Electronic transport by non-equilibrium Green function
- Electronic polarization by the Berry phase formalism
- Maximally localized Wannier functions
- Effective screening medium method for biased system
- Reaction path search by the NEB method
- Band unfolding method
- STM image by the Tersoff-Hamann method
- etc.

History of OpenMX

2000 Start of development

2003 Public release (GNU-GPL)

2003 Collaboration:
AIST, NIMS, SNU
KAIST, JAIST,
Kanazawa Univ.
CAS, UAM
NISSAN, Fujitsu Labs.
etc.

2019 19 public releases
Latest version: 3.9

http://www.openmx-square.org

Development of OpenMX code

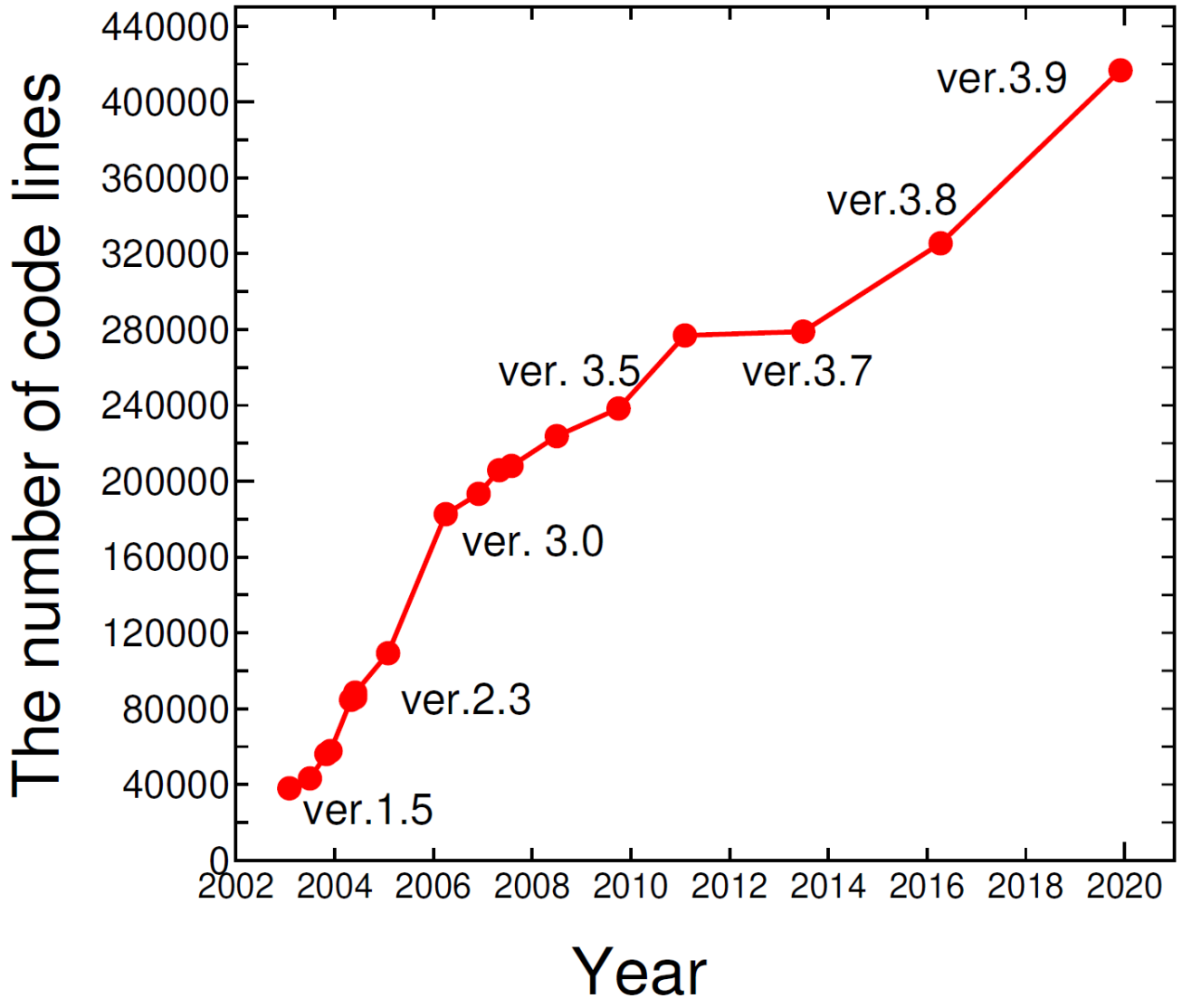

Contributors to OpenMX development

T. Ozaki (Univ. of Tokyo)
H. Kino (NIMS)
J. Yu (SNU)
M.J. Han (KAIST)
M. Ohfuchi (Fujitsu Labs.)
F. Ishii (Kanazawa Univ.)
K. Sawada (Kanazawa Univ.)
Y. Kubota (Kanazawa Univ.)
Y.P. Mizuta (Kanazawa Univ.)
H. Kotaka (Kyoto Univ.)
N. Yamaguchi (Kanazawa Univ.)
H. Sawahata (Kanazawa Univ.)
T.B. Prayitno (Kanazawa Univ.)
T. Ohwaki (NISSAN ARC)
T.V.T Duy (AISIN SEIKI)
M. Miyata (JAIST)
G. Jiang (Wuhan Univ. of Sci.&Tech.)
T. Iitaka (RIKEN)

P.-H. Chang (George Mason Univ.)
A. Terasawa (TIT)
Y. Gohda (TIT)
H. Weng (CAS)
Y. Shiihara (Toyota Tech. Inst.)
M. Toyoda (Tokyo Inst. Tech.)
Y. Okuno (FUJIFILM)
R. Perez (UAM)
P.P. Bell (UAM)
M. Ellner (UAM)
Yang Xiao (NUAA)
A.M. Ito (NIFS)
M. Otani (AIST)
M. Kawamura (Univ. of Tokyo)
K. Yoshimi (Univ. of Tokyo)
C.-C. Lee (Tamkang Univ.)
Y.-T. Lee (Academia Sinica)
M. Fukuda (Univ. of Tokyo)
S. Ryee (KAIST)
K. Terakura (AIST)

Materials studied by OpenMX

First characterization of silicene on ZrB_2 in collaboration with experimental groups

A. Fleurence et al., Phys. Rev. Lett. 108, 245501 (2012).

First identification of Jeff=1/2 Mott state of Ir oxides

B.J. Kim et al., Phys. Rev. Lett. 101, 076402 (2008).

Theoretical proposal of topological insulators

C.-H. Kim et al., Phys. Rev. Lett. 108, 106401 (2012).
H. Weng et al., Phy. Rev. X 4, 011002 (2014).

First-principles molecular dynamics simulations for Li ion battery

T. Ohwaki et al., J. Chem. Phys. 136, 134101 (2012).
T. Ohwaki et al., J. Chem. Phys. 140, 244105 (2014).

Magnetic anisotropy energy of magnets

Z. Torbatian et al., Appl. Phys. Lett. 104, 242403 (2014).
I. Kitagawa et al., Phys. Rev. B 81, 214408 (2010).

Electronic transport of graphene nanoribbon on surface oxidized Si

H. Jippo et al., Appl. Phys. Express 7, 025101 (2014).
M. Ohfuchi et al., Appl. Phys. Express 4, 095101 (2011).

Interface structures of carbide precipitate in bcc-Fe

H. Sawada et al., Modelling Simul. Mater. Sci. Eng. 21, 045012 (2013).

Universality of medium range ordered structure in amorphous metal oxides

K. Nishio et al., Phys. Rev. Lett. 340, 155502 (2013).

Materials treated so far

Silicene, graphene
Carbon nanotubes
Transition metal oxides
Topological insulators
Intermetallic compounds
Molecular magnets
Rare earth magnets
Lithium ion related materials
Structural materials
etc.

About 800 published papers

Silicene on ZrB_2

The XPS data is well compared with the calculated binding energy of planar-like structure.

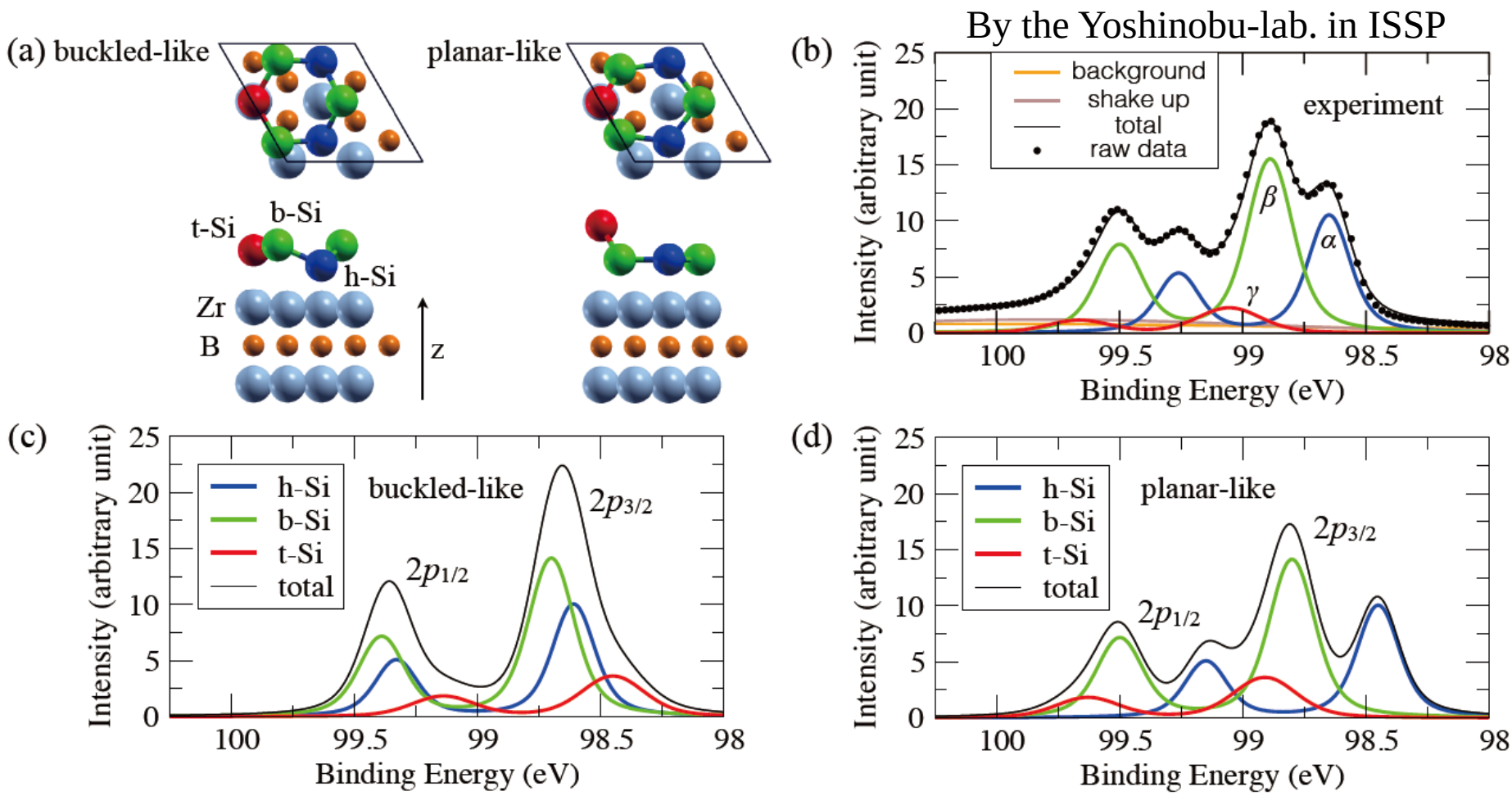

C.-C. Lee et al., PRB 95, 115437 (2017).

Electron transport of graphene nanoribbon

The NEGF calculations predict that the on/off ratio of conductance of the graphene nanoribbon on surface oxidized Si substrates is about 10^5, being consistent with experimental measurements.

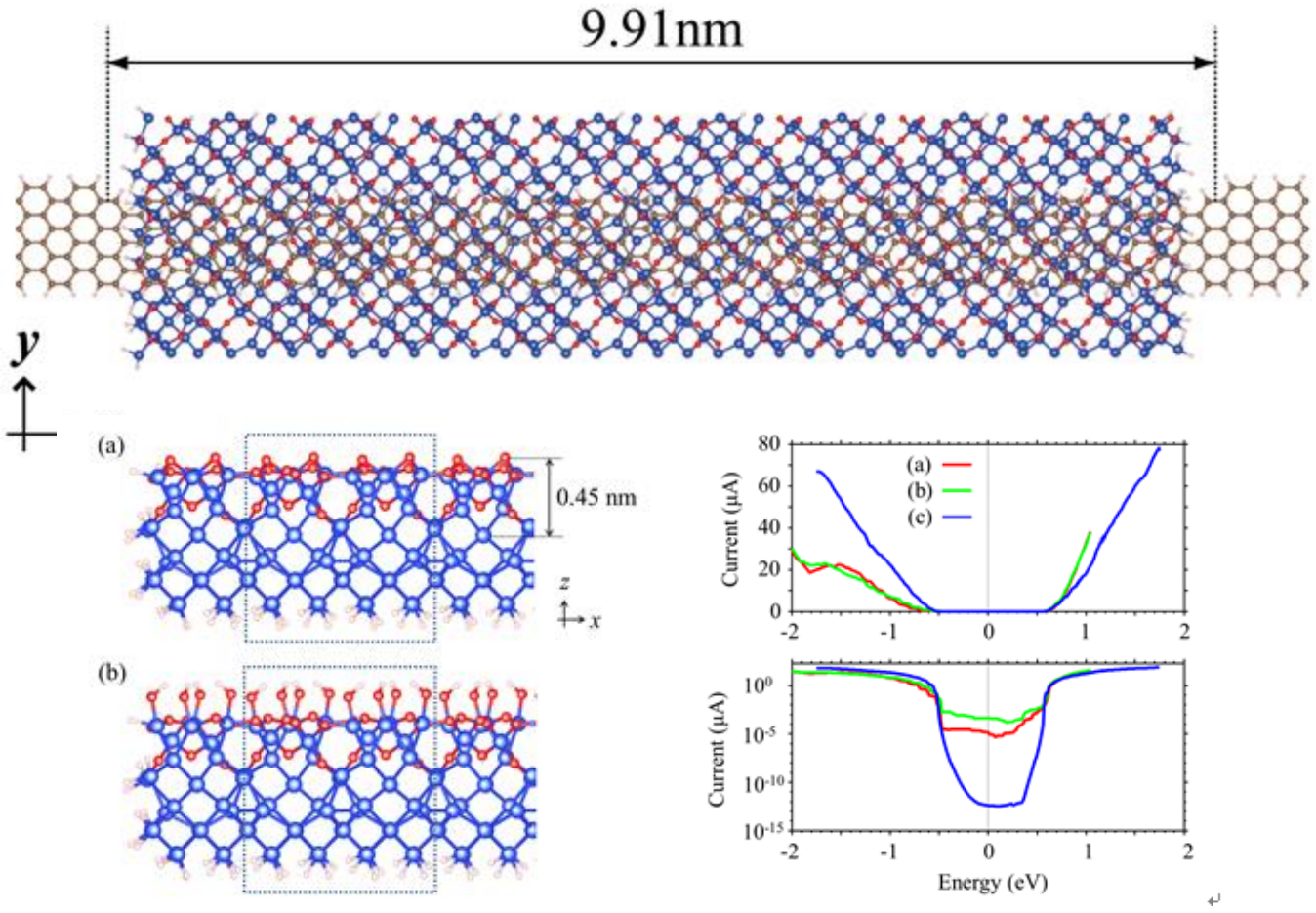

M. Ohfuchi et al., Appl. Phys. Express 4, 095101 (2011).

Interface of BCC-iron and metal carbides

The precipitation of metal carbides is an effective way to control the hardness and toughness of steel. We tried to estimate possible interface structures depending on the size of precipitates.

H. Sawada et al., Modelling Simul. Mater. Sci. Eng. 21, 045012 (2013).

HRTEM image

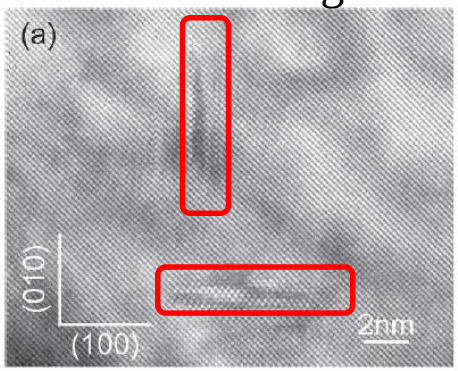

Precipitates: TiC, VC, NbC

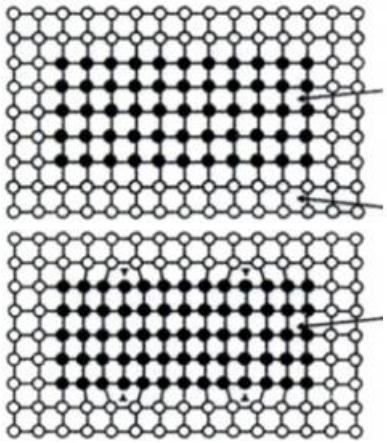

Coherent interface

BCC Fe

Semi-coherent interface

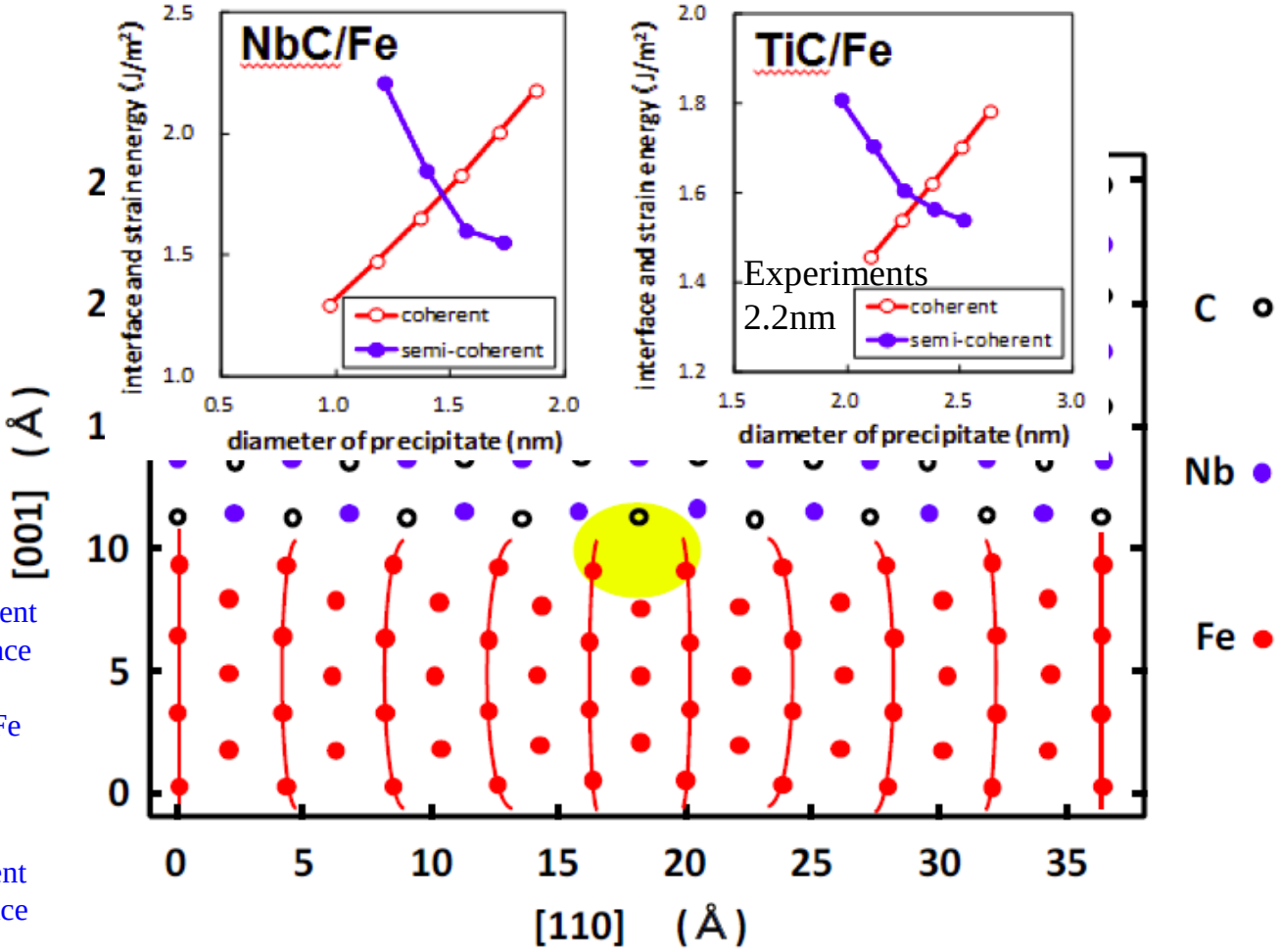

Implementation of OpenMX

- Density functional theory
- Mathematical structure of KS eq.
- LCPAO method
- Total energy
- Pseudopotentials
- Basis functions

Density functional theory

The energy of non-degenerate ground state can be expressed by a functional of electron density. (Hohenberg and Kohn, 1964)

$$E[\rho] = \int \rho(\mathbf{r}) v(\mathbf{r}) d + T[\rho] + J[\rho] + E_{\mathrm{xc}}[\rho]$$

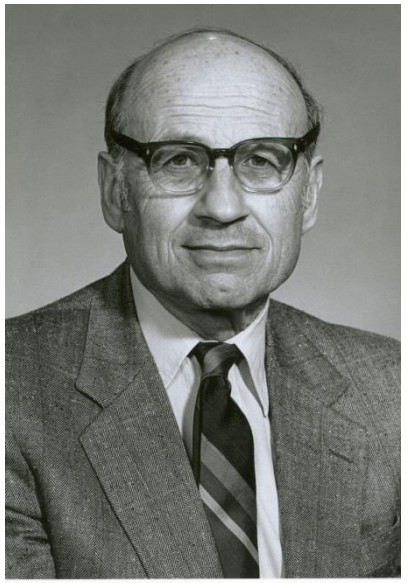

W.Kohn (1923-2016)

The many body problem of the ground state can be reduced to an one-particle problem with an effective potential. (Kohn-Sham, 1965)

$$\hat{H}_{\mathrm{KS}} \phi_i = \varepsilon_i \phi_i$$

$$\hat{H}_{\mathrm{KS}} = -\frac{1}{2}\nabla^2 + v_{\mathrm{eff}}$$

$$v_{\mathrm{eff}} = v_{\mathrm{ext}}(\mathbf{r}) + v_{\mathrm{Hartree}}(\mathbf{r}) + \frac{\delta E_{\mathrm{xc}}}{\delta \rho(\mathbf{r})}$$

Algorithmic structure of KS eq.

3D coupled non-linear differential equations have to be solved self-consistently.

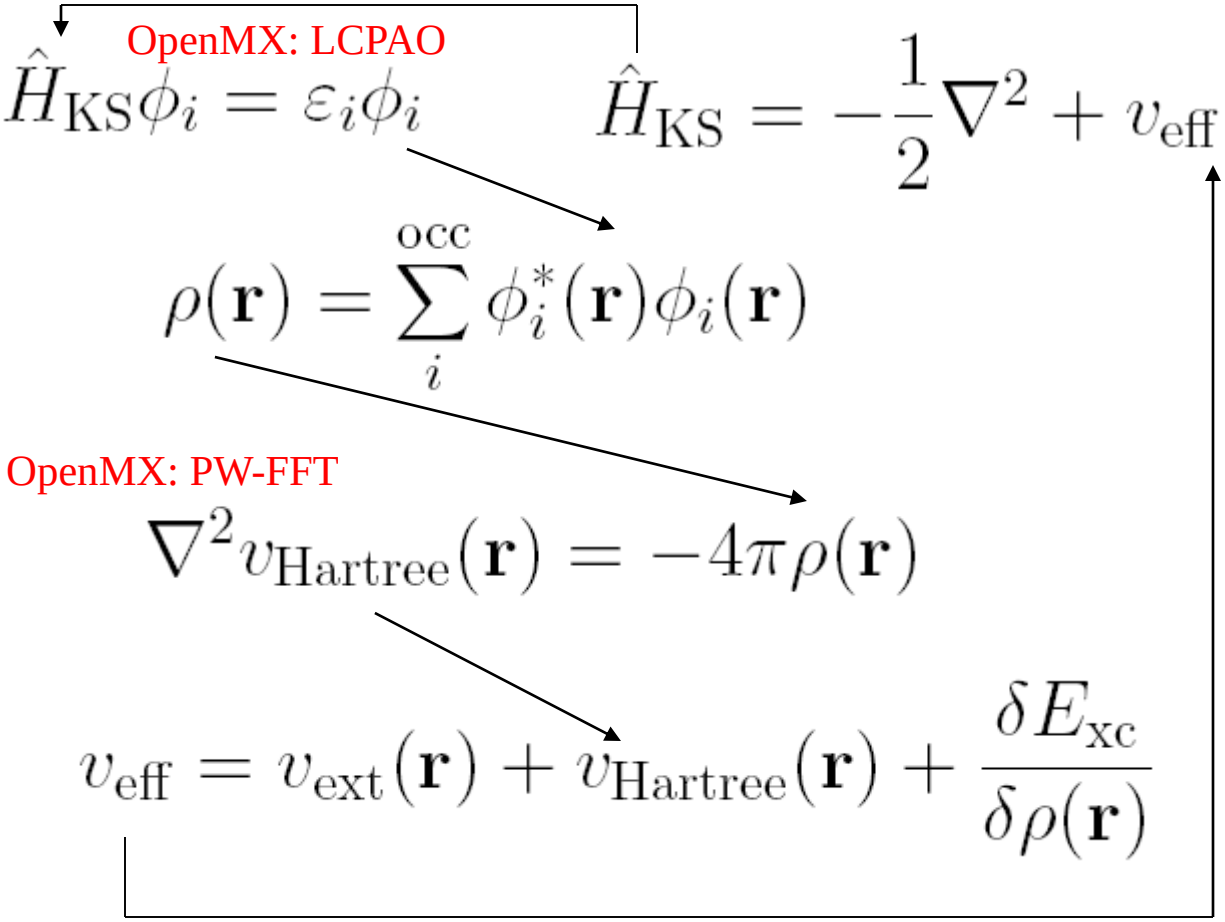

Input charge = Output charge → Self-consistent condition

LCPAO method

(Linear-Combination of Pseudo Atomic Orbital Method)

One-particle KS orbital

$$\psi_{\sigma\mu}^{(\mathbf{k})}(\mathbf{r}) = \frac{1}{\sqrt{N}} \sum_{\mathrm{n}}^{N} \mathrm{e}^{\mathrm{i}\mathbf{R}_{\mathrm{n}}\cdot\mathbf{k}} \sum_{i\alpha} c_{\sigma\mu,i\alpha}^{(\mathbf{k})} \phi_{i\alpha}(\mathbf{r} - \tau_i - \mathbf{R}_{\mathrm{n}}),$$

is expressed by a linear combination of atomic like orbitals in the method.

$$\phi(\mathbf{r}) = Y_l^m(\hat{\mathbf{r}})R(r)$$

Features:

- It is easy to interpret physical and chemical meanings, since the KS orbitals are expressed by the atomic like basis functions.
- It gives rapid convergent results with respect to basis functions due to physical origin. (however, it is not a complete basis set, leading to difficulty in getting full convergence.)
- The memory and computational effort for calculation of matrix elements are O(N).
- It well matches the idea of linear scaling methods.

- Total energy
- Pseudopotentials
- Basis functions

Implementation: Total energy (1)

The total energy is given by the sum of six terms, and a proper integration scheme for each term is applied to accurately evaluate the total energy.

$$E_{\rm tot} = E_{\rm kin} + E_{\rm ec} + E_{\rm ee} + E_{\rm xc} + E_{\rm cc} = E_{\rm kin} + E_{\rm na} + E_{\rm ec}^{\rm (NL)} + E_{\delta\rm ee} + E_{\rm xc} + E_{\rm scc}.$$

$$E_{\rm kin} = \sum_{\sigma}\sum_{\rm n}^{N}\sum_{i\alpha,j\beta}\rho_{\sigma,i\alpha j\beta}^{(\mathbf{R}_{\rm n})}h_{i\alpha j\beta,{\rm kin}}^{(\mathbf{R}_{\rm n})}.$$ Kinetic energy

$$E_{\rm ec} = E_{\rm ec}^{\rm (L)} + E_{\rm ec}^{\rm (NL)},$$ Coulomb energy with external potential

$$= \sum_{\sigma}\sum_{\rm n}^{N}\sum_{i\alpha,j\beta}\rho_{\sigma,i\alpha j\beta}^{(\mathbf{R}_{\rm n})}\langle\phi_{i\alpha}(\mathbf{r}-\tau_i)|\sum_I V_{{\rm core},I}(\mathbf{r}-\tau_I)|\phi_{j\beta}(\mathbf{r}-\tau_j-\mathbf{R}_{\rm n})\rangle$$

$$+ \sum_{\sigma}\sum_{\rm n}^{N}\sum_{i\alpha,j\beta}\rho_{\sigma,i\alpha j\beta}^{(\mathbf{R}_{\rm n})}\langle\phi_{i\alpha}(\mathbf{r}-\tau_i)|\sum_I V_{{\rm NL},I}(\mathbf{r}-\tau_I)|\phi_{j\beta}(\mathbf{r}-\tau_j-\mathbf{R}_{\rm n})\rangle,$$

$$E_{\rm ee} = \frac{1}{2}\int dr^3 n(\mathbf{r})V_{\rm H}(\mathbf{r}),$$ Hartree energy

$$= \frac{1}{2}\int dr^3 n(\mathbf{r})\{V_{\rm H}^{\rm (a)}(\mathbf{r}) + \delta V_{\rm H}(\mathbf{r})\},$$

$$E_{\rm xc} = \int dr^3\{n_\uparrow(\mathbf{r}) + n_\downarrow(\mathbf{r}) + n_{\rm pcc}(\mathbf{r})\}\epsilon_{\rm xc}(n_\uparrow + \frac{1}{2}n_{\rm pcc}, n_\downarrow + \frac{1}{2}n_{\rm pcc}),$$ Exchange-correlation energy

$$E_{\rm cc} = \frac{1}{2}\sum_{I,J}\frac{Z_I Z_J}{|\tau_I - \tau_J|}.$$ Core-core Coulomb energy

TO and H.Kino, PRB 72, 045121 (2005)

Implementation: Total energy (2)

The reorganization of Coulomb energies gives three new energy terms.

$$E_{\rm ec}^{(L)} + E_{\rm ee} + E_{\rm cc} = E_{\rm na} + E_{\delta\rm ee} + E_{\rm scc},$$

The neutral atom energy

$$\begin{aligned} E_{\rm na} &= \int dr^3 n(\mathbf{r}) \sum_I V_{{\rm na},I}(\mathbf{r}-\tau_I), \\ &= \sum_\sigma \sum_{\rm n}^{N} \sum_{i\alpha,j\beta} \rho_{\sigma,i\alpha j\beta}^{(\mathbf{R_n})} \sum_I \langle \phi_{i\alpha}(\mathbf{r}-\tau_i) | V_{{\rm na},I}(\mathbf{r}-\tau_I) | \phi_{j\beta}(\mathbf{r}-\tau_j-\mathbf{R}_{\rm n}) \rangle, \end{aligned}$$

Short range and separable to two-center integrals

Difference charge Hartree energy

$$E_{\delta\rm ee} = \frac{1}{2}\int dr^3 \delta n(\mathbf{r}) \delta V_{\rm H}(\mathbf{r}),$$

Long range but minor contribution

Screened core-core repulsion energy

$$E_{\rm scc} = \frac{1}{2}\sum_{I,J}\left[\frac{Z_I Z_J}{|\tau_I-\tau_J|} - \int dr^3 n_I^{(\rm a)}(\mathbf{r}) V_{{\rm H},J}^{(\rm a)}(\mathbf{r})\right].$$

Short range and two-center integrals

Difference charge

$$\begin{aligned} \delta n(\mathbf{r}) &= n(\mathbf{r}) - n^{(\rm a)}(\mathbf{r}), \\ &= n(\mathbf{r}) - \sum_i n_i^{(\rm a)}(\mathbf{r}), \end{aligned}$$

Neutral atom potential

$$V_{{\rm na},I}(\mathbf{r}-\tau_I) = V_{{\rm core},I}(\mathbf{r}-\tau_I) + V_{{\rm H},I}^{(\rm a)}(\mathbf{r}-\tau_I).$$

Implementation: Total energy (3)

So, the total energy is given by

$$E_{\mathrm{tot}} = E_{\mathrm{kin}} + E_{\mathrm{na}} + E_{\mathrm{ec}}^{(\mathrm{NL})} + E_{\delta\mathrm{ee}} + E_{\mathrm{xc}} + E_{\mathrm{scc}}.$$

Each term is evaluated by using a different numerical grid with consideration on accuracy and efficiency.

E_{kin}
E_{na} } Spherical coordinate in momentum space
$E_{\mathrm{ec}}^{(\mathrm{NL})}$

$E_{\delta\mathrm{ee}}$
E_{xc} } Real space regular mesh

E_{scc} Real space fine mesh

Two center integrals

Fourier-transformation of basis functions

$$
\begin{aligned}
\tilde{\phi}_{i\alpha}(\mathbf{k}) &= \left(\frac{1}{\sqrt{2\pi}}\right)^3 \int dr^3 \phi_{i\alpha}(\mathbf{r}) \mathrm{e}^{-\mathrm{i}\mathbf{k}\cdot\mathbf{r}} \\
&= \left(\frac{1}{\sqrt{2\pi}}\right)^3 \int dr^3 Y_{lm}(\hat{\mathbf{r}}) R_{pl}(r) \left\{ 4\pi \sum_{L=0}^{\infty} \sum_{M=-L}^{L} (-\mathrm{i})^L j_L(kr) Y_{LM}(\hat{\mathbf{k}}) Y^*_{LM}(\hat{\mathbf{r}}) \right\}, \\
&= \left(\frac{1}{\sqrt{2\pi}}\right)^3 4\pi \sum_{L=0}^{\infty} \sum_{M=-L}^{L} (-\mathrm{i})^L Y_{LM}(\hat{\mathbf{k}}) \int dr r^2 R_{pl}(r) j_L(kr) \int d\theta d\phi \sin(\theta) Y_{lm}(\hat{\mathbf{r}}) Y^*_{LM}(\hat{\mathbf{r}}), \\
&= \left[\left(\frac{1}{\sqrt{2\pi}}\right)^3 4\pi (-\mathrm{i})^l \int dr r^2 R_{pl}(r) j_L(kr) \right] Y_{lm}(\hat{\mathbf{k}}), \\
&= \tilde{R}_{pl}(k) Y_{lm}(\hat{\mathbf{k}}),
\end{aligned}
$$

Integrals for angular parts are analytically performed. Thus, we only have to perform one-dimensional integrals along the radial direction.

e.g., overlap integral

$$
\begin{aligned}
\langle \phi_{i\alpha}(\mathbf{r}) | \phi_{j\beta}(\mathbf{r}-\tau) \rangle &= \int dr^3 \phi^*_{i\alpha}(\mathbf{r}) \phi_{j\beta}(\mathbf{r}-\tau), \\
&= \int dr^3 \left(\frac{1}{\sqrt{2\pi}}\right)^3 \int dk^3 \tilde{R}^*_{pl}(k) Y^*_{lm}(\hat{\mathbf{k}}) \mathrm{e}^{-\mathrm{i}\mathbf{k}\cdot\mathbf{r}} \left(\frac{1}{\sqrt{2\pi}}\right)^3 \int dk'^3 \tilde{R}_{p'l'}(k') Y_{l'm'}(\hat{\mathbf{k}}') \mathrm{e}^{\mathrm{i}\mathbf{k}'\cdot(\mathbf{r}-\tau)}, \\
&= \left(\frac{1}{2\pi}\right)^3 \int dk^3 \int dk'^3 \mathrm{e}^{-\mathrm{i}\mathbf{k}'\cdot\tau} \tilde{R}^*_{pl}(k) Y^*_{lm}(\hat{\mathbf{k}}) \tilde{R}_{p'l'}(k') Y_{l'm'}(\hat{\mathbf{k}}') \int dr^3 \mathrm{e}^{\mathrm{i}(\mathbf{k}'-\mathbf{k})\cdot\mathbf{r}}, \\
&= \int dk^3 \mathrm{e}^{-\mathrm{i}\mathbf{k}\cdot\tau} \tilde{R}^*_{pl}(k) Y^*_{lm}(\hat{\mathbf{k}}) \tilde{R}_{p'l'}(k) Y_{l'm'}(\hat{\mathbf{k}}),
\end{aligned}
$$

Cutoff energy for regular mesh

The two energy components $E_{\delta ee} + E_{xc}$ are calculated on real space regular mesh. The mesh fineness is determined by plane-wave cutoff energies.

```
scf.energycutoff          150.0          # default=150 (Ry)
```

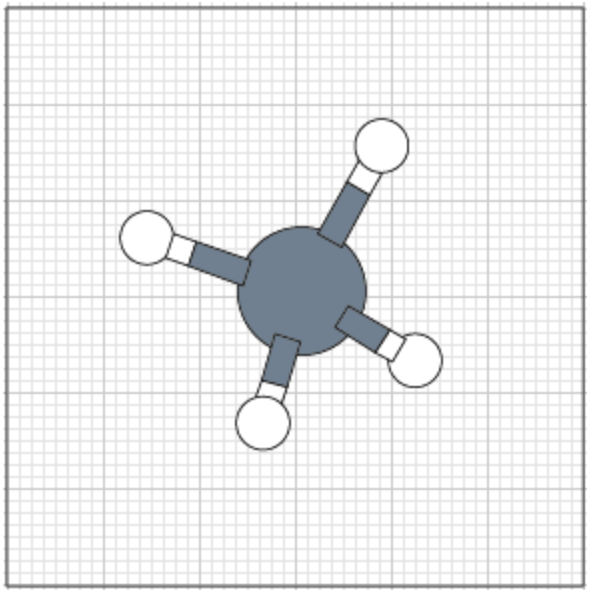

The cutoff energy can be related to the mesh fineness by the following eqs.

$$E_{\rm cut}^{(1)} = \frac{1}{2}\mathbf{gb}_1 \cdot \mathbf{gb}_1, \quad E_{\rm cut}^{(2)} = \frac{1}{2}\mathbf{gb}_2 \cdot \mathbf{gb}_2, \quad E_{\rm cut}^{(3)} = \frac{1}{2}\mathbf{gb}_3 \cdot \mathbf{gb}_3,$$

$$\mathbf{ga}_1 = \frac{\mathbf{a}_1}{N_1}, \quad \mathbf{ga}_2 = \frac{\mathbf{a}_2}{N_2}, \quad \mathbf{ga}_3 = \frac{\mathbf{a}_3}{N_3},$$

$$\mathbf{gb}_1 = 2\pi\frac{\mathbf{ga}_2 \times \mathbf{ga}_2}{\Delta V}, \quad \mathbf{gb}_2 = 2\pi\frac{\mathbf{ga}_3 \times \mathbf{ga}_1}{\Delta V}, \quad \mathbf{gb}_2 = 2\pi\frac{\mathbf{ga}_1 \times \mathbf{ga}_2}{\Delta V},$$

$$\Delta V = \mathbf{ga}_1 \cdot (\mathbf{ga}_2 \times \mathbf{ga}_3),$$

Forces

$$\mathbf{F}_i = -\frac{\partial E_{\rm tot}}{\partial \mathbf{R}_i} = -\frac{\partial E_{\rm kin}}{\partial \mathbf{R}_i} - \frac{\partial E_{\rm na}}{\partial \mathbf{R}_i} - \frac{\partial E_{\rm scc}}{\partial \mathbf{R}_i} - \frac{\partial E_{\delta \rm ee}}{\partial \mathbf{R}_i} - \frac{\partial E_{\rm xc}}{\partial \mathbf{R}_i} - \frac{\partial E_{\rm cc}}{\partial \mathbf{R}_i}$$

$$\frac{\partial E_{\delta \rm ee}}{\partial \mathbf{R}_k} = \sum_{\rm p} \frac{\partial n(\mathbf{r}_{\rm p})}{\partial \mathbf{R}_k} \frac{\partial E_{\delta \rm ee}}{\partial n(\mathbf{r}_{\rm p})} + \sum_{\rm p} \frac{\partial n^{\rm a}(\mathbf{r}_{\rm p})}{\partial \mathbf{R}_k} \frac{\partial E_{\delta \rm ee}}{\partial n^{\rm a}(\mathbf{r}_{\rm p})}.$$

$$\begin{aligned}
\frac{\partial E_{\delta \rm ee}}{\partial n(\mathbf{r}_{\rm p})} &= \frac{1}{2}\Delta V \{\delta V_{\rm H}(\mathbf{r}_{\rm p}) + \sum_{\rm q} \delta n(\mathbf{r}_{\rm q}) \frac{\partial \delta V_{\rm H}(\mathbf{r}_{\rm q})}{\partial n(\mathbf{r}_{\rm p})}\}, \\
&= \frac{1}{2}\Delta V \{\delta V_{\rm H}(\mathbf{r}_{\rm p}) + \frac{4\pi}{N_{\rm rsg}} \sum_{\rm G} \frac{1}{|\mathbf{G}|^2} \sum_{\rm q} \delta n(\mathbf{r}_{\rm q}) e^{i\mathbf{G}\cdot(\mathbf{r}_{\rm q}-\mathbf{r}_{\rm p})}\}, \\
&= \Delta V \delta V_{\rm H}(\mathbf{r}_{\rm p}).
\end{aligned}$$

$$\begin{aligned}
\frac{\partial E_{\delta \rm ee}}{\partial n^{\rm a}(\mathbf{r}_{\rm p})} &= -\frac{1}{2}\Delta V \{\delta V_{\rm H}(\mathbf{r}_{\rm p}) - \sum_{\rm q} \delta n(\mathbf{r}_{\rm q}) \frac{\partial \delta V_{\rm H}(\mathbf{r}_{\rm q})}{\partial n^{\rm a}(\mathbf{r}_{\rm p})}\}, \\
&= -\frac{1}{2}\Delta V \{\delta V_{\rm H}(\mathbf{r}_{\rm p}) + \frac{4\pi}{N_{\rm rsg}} \sum_{\rm G} \frac{1}{|\mathbf{G}|^2} \sum_{\rm q} \delta n(\mathbf{r}_{\rm q}) e^{i\mathbf{G}\cdot(\mathbf{r}_{\rm q}-\mathbf{r}_{\rm p})}\}, \\
&= -\Delta V \delta V_{\rm H}(\mathbf{r}_{\rm p}).
\end{aligned}$$

$$\begin{aligned}
\frac{\partial n(\mathbf{r}_{\rm p})}{\partial \mathbf{R}_k} &= \sum_{i\alpha,j\beta} \sum_{\nu} \{\frac{\partial c^*_{i\alpha,\nu}}{\partial \mathbf{R}_k} c_{j\beta,\nu} \chi_{i\alpha}(\mathbf{r}) \chi_{j\beta}(\mathbf{r}) + c^*_{i\alpha,\nu} \frac{\partial c_{j\beta,\nu}}{\partial \mathbf{R}_k} \chi_{i\alpha}(\mathbf{r}_{\rm p}) \chi_{j\beta}(\mathbf{r}_{\rm p})\} \\
&\quad + 2 \sum_{\alpha,j\beta} \rho_{k\alpha,j\beta} \frac{\partial \chi_{k\alpha}(\mathbf{r}_{\rm p})}{\partial \mathbf{R}_k} \chi_{j\beta}(\mathbf{r}_{\rm p}).
\end{aligned}$$

$$\begin{aligned}
\frac{\partial E_{\rm xc}}{\partial \mathbf{R}_k} &= \sum_{\rm p} \frac{\partial n(\mathbf{r}_{\rm p})}{\partial \mathbf{R}_k} \frac{\partial E_{\rm xc}}{\partial n(\mathbf{r}_{\rm p})}, \\
&= \Delta V \sum_{\rm p} \frac{\partial n(\mathbf{r}_{\rm p})}{\partial \mathbf{R}_k} v_{\rm xc}(n(\mathbf{r}_{\rm p})).
\end{aligned}$$

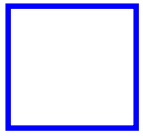

Easy calc.

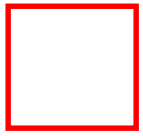

See the left

Forces are always analytic at any grid fineness and at zero temperature, even if numerical basis functions and numerical grids.

- Total energy
- Pseudopotentials
- Basis functions

Norm-conserving Vanderbilt pseudopotential

I. Morrion, D.M. Bylander, and L. Kleinman, PRB 47, 6728 (1993).

The following non-local operator proposed by Vanderbilt guarantees that scattering properties are reproduced around multiple reference energies.

D. Vanderbilt, PRB 41, 7892 (1990).

$$V_{\mathrm{NL}} = \sum_{i,j} B_{ij} |\beta_i\rangle\langle\beta_j|$$

$$|\chi_i\rangle = V_{\mathrm{NL}}^{(i)} |\phi_i\rangle = (\varepsilon_i - T - V_{\mathrm{loc}})|\phi_i\rangle$$

$$B_{ij} = \langle\phi_i|\chi_j\rangle$$

$$|\beta_i\rangle = \sum_j (B^{-1})_{ji} |\chi_j\rangle$$

If the following generalized norm-conserving condition is fulfilled, the matrix B is Hermitian, resulting in that V_{NL} is also Hermitian.

$$Q_{ij} = \langle\psi_i|\psi_j\rangle_R - \langle\phi_i|\phi_j\rangle_R$$

If Q=0, then B-B*=0

$$B_{ij} - B_{ji}^* = (\varepsilon_i - \varepsilon_j) Q_{ij}$$

This is the norm-conserving PP used in OpenMX

Non-local potentials by Vanderbilt

Let's operate the non-local potential on a pseudized wave function:

$$
\begin{aligned}
\hat{v}^{(\mathrm{NL})}|\phi_k^{(\mathrm{PS})}\rangle &= \sum_{ij} |\beta_i\rangle B_{ij} \langle\beta_j|\phi_k^{(\mathrm{PS})}\rangle \\
&= \sum_{ij} |\beta_i\rangle B_{ij} \sum_{k'} \left(B^{-1}\right)_{k'j} \langle\chi_{k'}|\phi_k^{(\mathrm{PS})}\rangle, \\
&= \sum_{ij} |\beta_i\rangle B_{ij} \sum_{k'} \left(B^{-1}\right)_{k'j} B_{kk'}, \\
&= \sum_{ij} |\beta_i\rangle B_{ij} \delta_{kj}, \\
&= \sum_{i} \left(\sum_{j} \left(B^{-1}\right)_{ji} |\chi_j\rangle \right) B_{ik}. \\
&= |\chi_k\rangle
\end{aligned}
$$

Noting the following relations:

$$v^{(\mathrm{SL})}(r) = v_{\mathrm{L}}(r) + v_{\mathrm{H}}^{(\mathrm{v})}(r) + v_{\mathrm{xc}}^{(\mathrm{v+pcc})}(r).$$

$$|\chi_i\rangle = \left(\varepsilon_i + \frac{1}{2}\nabla^2 - v^{(\mathrm{SL})}(r)\right)|\phi_i^{(\mathrm{PS})}\rangle,$$

$$B_{ij} = \langle\phi_i^{(\mathrm{PS})}|\chi_j\rangle$$

$$|\beta_i\rangle = \sum_j \left(B^{-1}\right)_{ji} |\chi_j\rangle.$$

It turns out that the following Schrodinger eq. is hold.

$$\left(-\frac{1}{2}\nabla^2 + v^{(\mathrm{SL})}(r) + \hat{v}^{(\mathrm{NL})}\right)|\phi_i^{(\mathrm{PS})}\rangle = \varepsilon_i |\phi_i^{(\mathrm{PS})}\rangle.$$

Generalized norm-conserving conditions Q_{ij}

In the Vanderbilt pseudopotential, B is given by

$$B_{ij} = \int_0^{r_c} dr P_i^{(\mathrm{PS})}(r) \left(\varepsilon_j + \frac{1}{2}\frac{d^2}{dr^2} - \frac{l(l+1)}{2r^2} - v^{(\mathrm{SL})}(r) \right) P_j^{(\mathrm{PS})}(r),$$

$$B_{ji}^* = \int_0^{r_c} dr P_i^{(\mathrm{PS})}(r) \left(\varepsilon_i + \frac{1}{2}\frac{d^2}{dr^2} - \frac{l(l+1)}{2r^2} - v^{(\mathrm{SL})}(r) \right) P_j^{(\mathrm{PS})}(r),$$

Thus, we have

$$B_{ij} - B_{ji}^* = (\varepsilon_j - \varepsilon_i) \int_0^{r_c} dr P_i^{(\mathrm{PS})}(r) P_j^{(\mathrm{PS})}(r)$$
$$+\frac{1}{2}\int_0^{r_c} dr P_i^{(\mathrm{PS})}(r) P_j''^{(\mathrm{PS})}(r) - \frac{1}{2}\int_0^{r_c} dr P_i''^{(\mathrm{PS})}(r) P_j^{(\mathrm{PS})}(r).$$

By integrating by parts, this can be transformed as

$$B_{ij} - B_{ji}^* = (\varepsilon_j - \varepsilon_i)\langle \phi_i^{(\mathrm{PS})} | \phi_j^{(\mathrm{PS})} \rangle_{r_c} + \frac{1}{2}\left[P_i^{(\mathrm{PS})}(r) P_j'^{(\mathrm{PS})}(r) \right]_0^{r_c} - \frac{1}{2}\left[P_i'^{(\mathrm{PS})}(r) P_j^{(\mathrm{PS})}(r) \right]_0^{r_c},$$
$$= (\varepsilon_j - \varepsilon_i)\langle \phi_i^{(\mathrm{PS})} | \phi_j^{(\mathrm{PS})} \rangle_{r_c} + \frac{1}{2} P_i^{(\mathrm{PS})}(r_c) P_j'^{(\mathrm{PS})}(r_c) - \frac{1}{2} P_i'^{(\mathrm{PS})}(r_c) P_j^{(\mathrm{PS})}(r_c). \quad \cdots (1)$$

As well, the similar calculations can be performed for all electron wave functions.

$$0 = (\varepsilon_j - \varepsilon_i)\langle \phi_i^{(\mathrm{AE})} | \phi_j^{(\mathrm{AE})} \rangle_{r_c} + \frac{1}{2} P_i^{(\mathrm{AE})}(r_c) P_j'^{(\mathrm{AE})}(r_c) - \frac{1}{2} P_i'^{(\mathrm{AE})}(r_c) P_j^{(\mathrm{AE})}(r_c). \quad \cdots (2)$$

By subtracting (2) from (1), we obtain a relation between B and Q.

$$B_{ij} - B_{ji}^* = (\varepsilon_i - \varepsilon_j)\left(\langle \phi_i^{(\mathrm{AE})} | \phi_j^{(\mathrm{AE})} \rangle_{r_c} - \langle \phi_i^{(\mathrm{PS})} | \phi_j^{(\mathrm{PS})} \rangle_{r_c} \right).$$

Norm-conserving pseudopotential by MBK

I. Morrion, D.M. Bylander, and L. Kleinman, PRB 47, 6728 (1993).

If $Q_{ij} = 0$, the non-local terms can be transformed to a diagonal form.

$$V_{\rm NL} = \sum_{i,j} B_{ij} |\beta_i\rangle\langle\beta_j|,$$
$$= \sum_{i} \lambda_i |\alpha_i\rangle\langle\alpha_i|$$

The form is equivalent to that obtained from the Blochl expansion for TM norm-conserving pseudopotentials. Thus, common routines can be utilized for the MBK and TM pseudopotentials, resulting in easiness of the code development.

To satisfy $Q_{ij}=0$, pseudofunctions are now given by

$$\phi_i = \phi_{{\rm TM},i} + f_i \quad f_i = \sum_{i=0} c_i \left[r j_l \left(\frac{r}{r_c} u_{li} \right) \right]$$

The coefficients {c} are determined by agreement of derivatives and $Q_{ij}=0$.
Once a set of {c} is determined, χ is given by

$$\chi_i = V_{\rm TM}^{(i)} \phi_{{\rm TM},i} + \varepsilon_i f_i - V_{\rm loc}\phi_i - \frac{1}{2}\sum_i c_i \left(\frac{u_{li}}{r_c} \right)^2 \left[r j_l \left(\frac{r}{r_c} u_{li} \right) \right]$$

Pseudo-wave funtion and psedopotential of carbon atom

Red: All electron calculation

Blue: Pseudized calculation

Pseudopotential for C 2s and –4/r

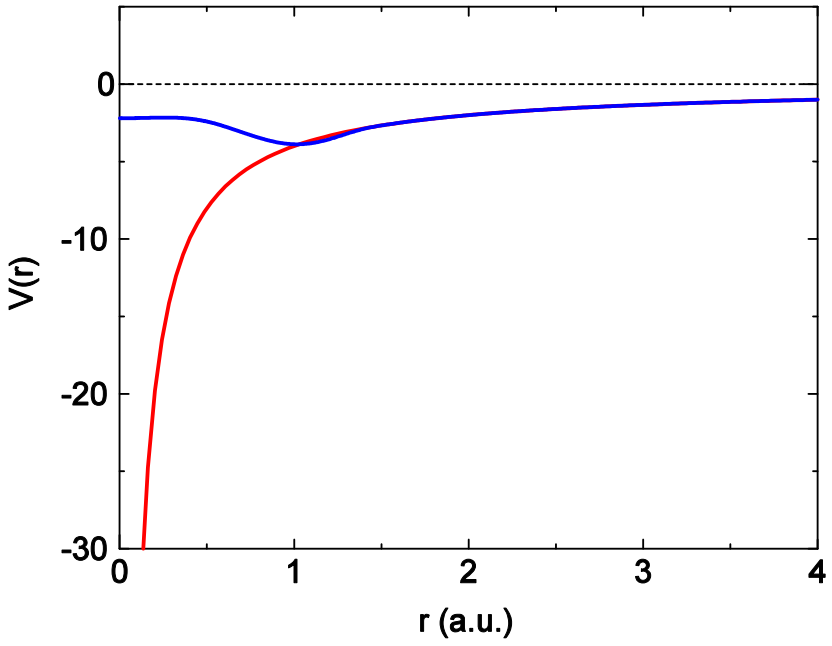

Radial wave function of C 2s

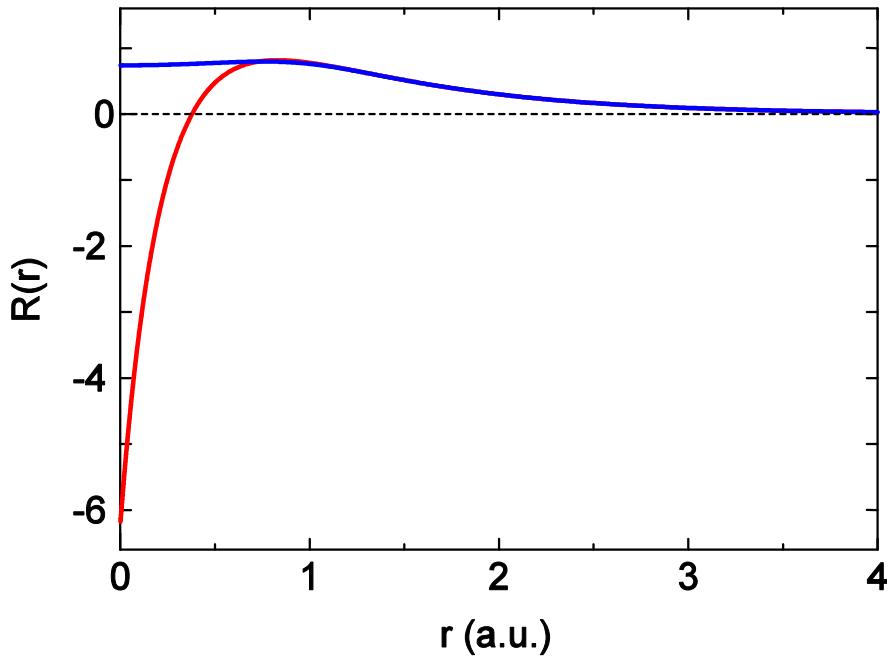

Optimization of pseudopotentials

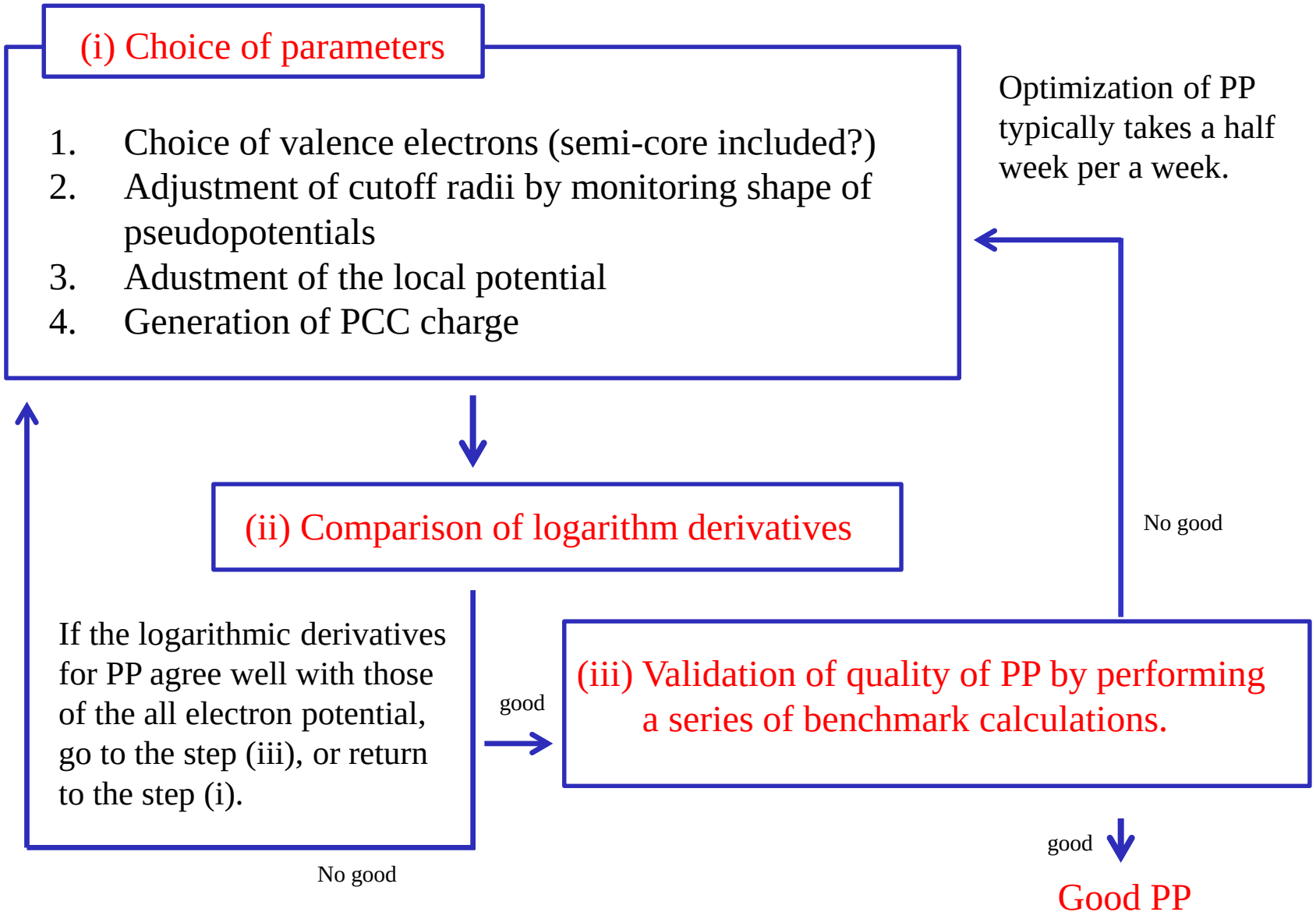

Comparison of logarithmic derivatives

Logarithmic derivatives of s, p, d, f channels for Mn. The deviation between PP and all electron directly affects the band structure.

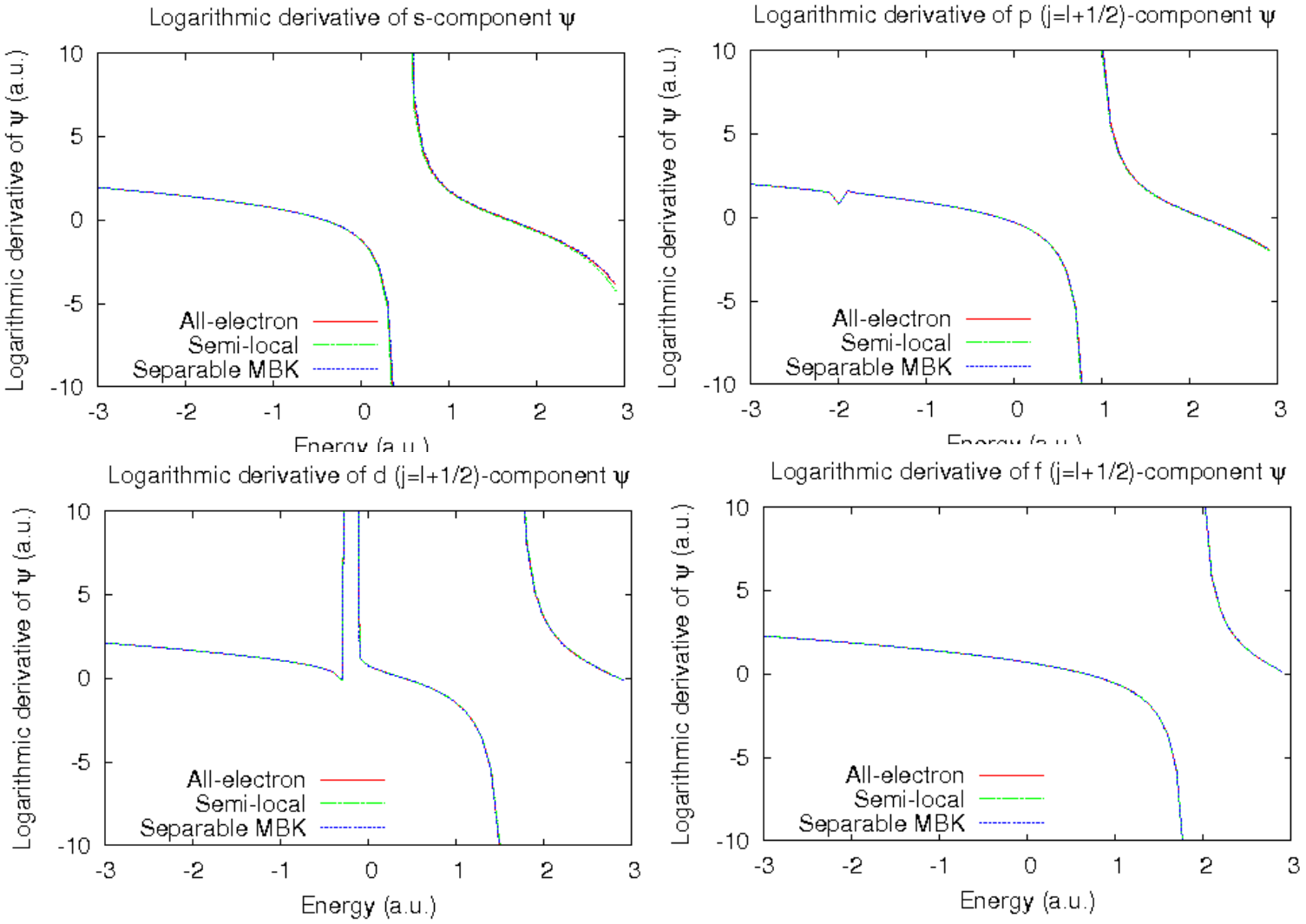

Comparison of band structure for fcc Mn

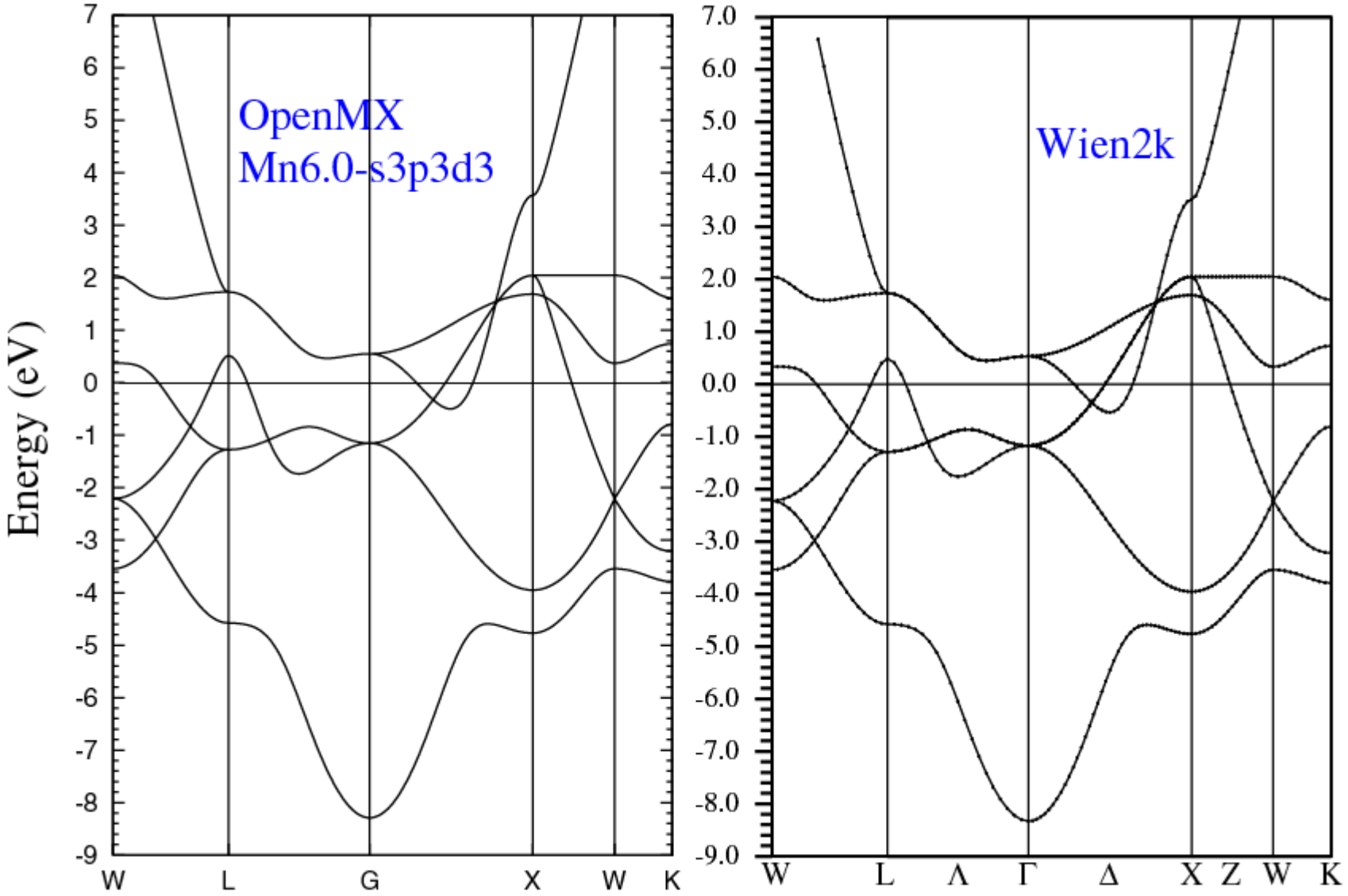

- Total energy
- Pseudopotentials
- Basis functions

Primitive basis functions

1. Solve an atomic Kohn-Sham eq. under a confinement potential:

$$V_{\text{core}}(r)=\begin{cases} -\dfrac{Z}{r} & \text{for } r\leqslant r_1 \\ \displaystyle\sum_{n=0}^{3} b_n r^n & \text{for } r_1<r\leqslant r_c \\ h & \text{for } r_c<r, \end{cases}$$

2. Construct the norm-conserving pseudopotentials.

3. Solve ground and excited states for the the peudopotential for each L-channel.

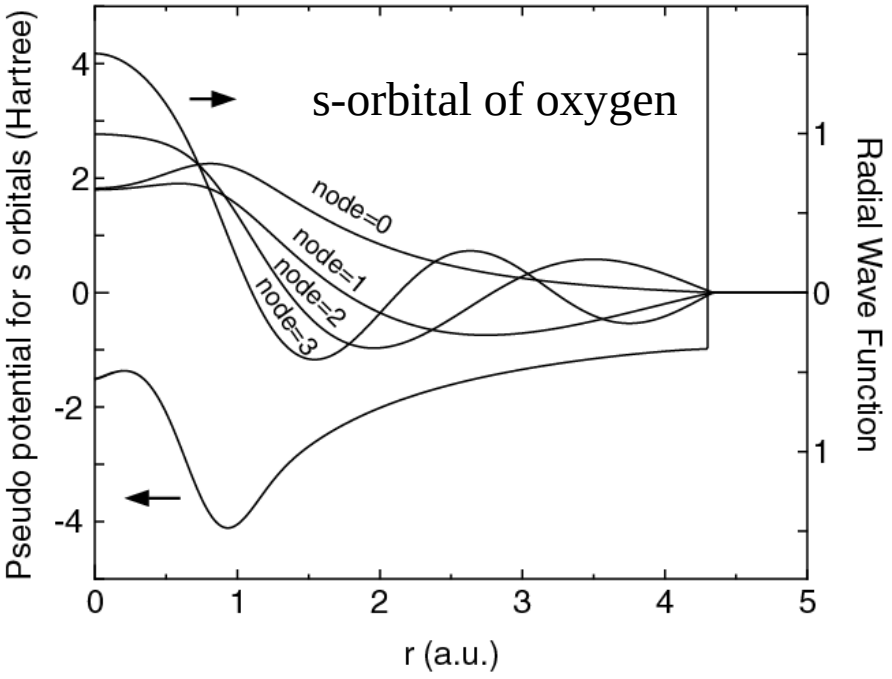

In most cases, the accuracy and efficiency can be controlled by

Cutoff radius

Number of orbitals

PRB 67, 155108 (2003)
PRB 69, 195113 (2004)

Convergence with respect to basis functions

The two parameters can be regarded as variational parameters.

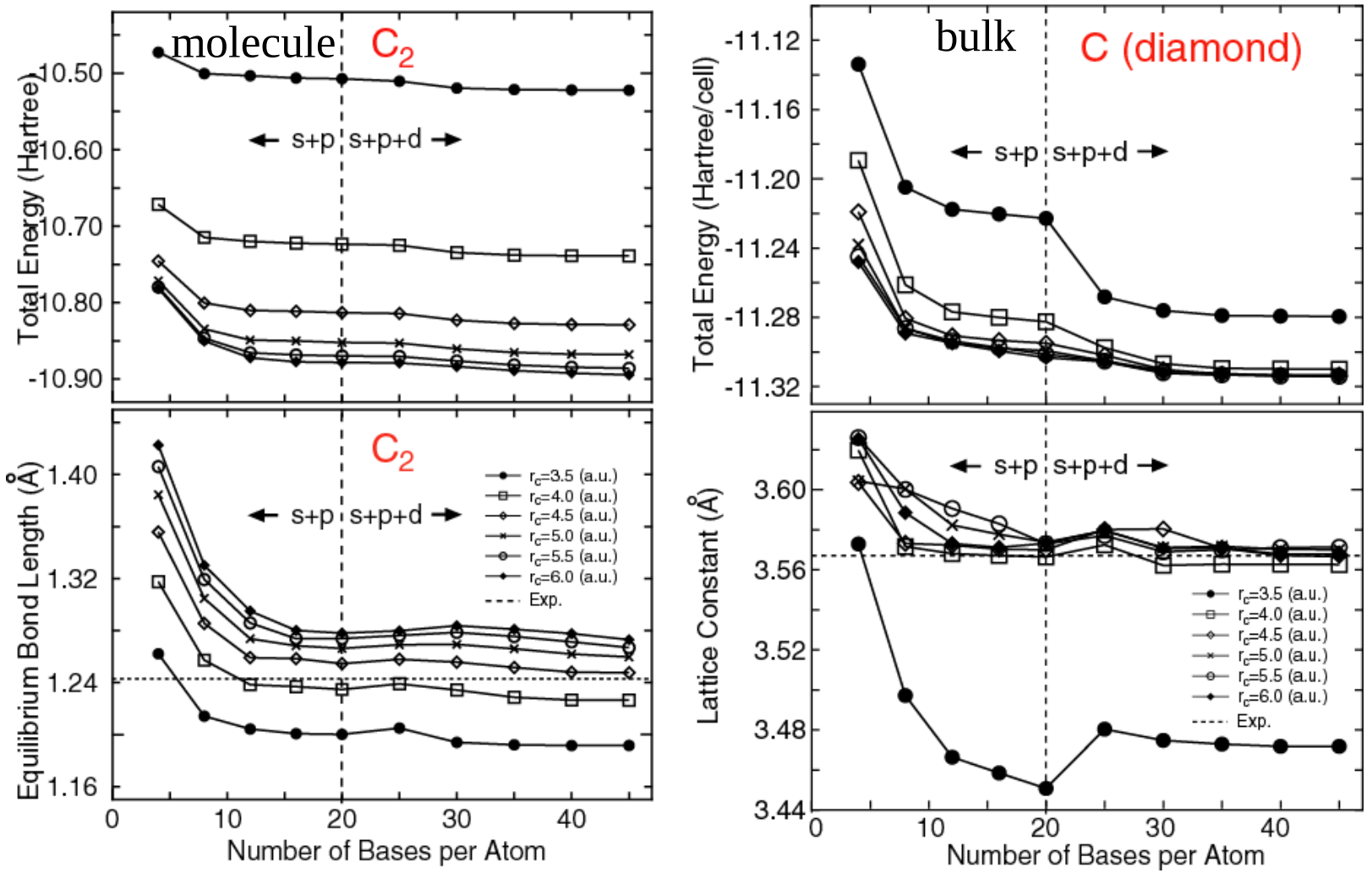

Benchmark of primitive basis functions

Ground state calculations of dimer using primitive basis functions

Dimer	Expt.	Calc.	Dimer	Expt.	Calc.
H_2 (H4.5-$s2$)	$^1\Sigma_g^+$ [a]	$^1\Sigma_g^+$ $(1s\sigma_g^2)$	K_2 (K10.0-$s2p2$)	$^1\Sigma_g^+$ [f]	$^1\Sigma_g^+$ $(3p\pi_g^4 3p\sigma_u^2 4s\sigma_g^2)$
He_2 (He7.0-$s2$)	$^1\Sigma_g^+$ [b]	$^1\Sigma_g^+$ $(1s\sigma_g^2 1s\sigma_u^2)$	CaO (Ca7.0-$s2p2d2$)	$^1\Sigma^+$ [k]	$^1\Sigma^+$ $(s\sigma^2 s\sigma^2 p\pi^4)$
Li_2 (Li8.0-$s2$)	$^1\Sigma_g^+$ [c]	$^1\Sigma_g^+$ $(2s\sigma_g^2)$	ScO (Sc7.0-$s2p2d2$)	$^2\Sigma^+$ [l]	$^2\Sigma^+$ $(d\pi^4 s\sigma^2 s\sigma^1)$
BeO (Be6.0-$s2p2$)	$^1\Sigma^+$ [d]	$^1\Sigma^+$ $(s\sigma^2 s\sigma^2 p\pi^4)$	Ti_2 (Ti7.0-$s2p2d2$)	$^3\Delta_g$ [m]	$^3\Delta_g$ $(4s\sigma_g^2 3d\sigma_g^1 3d\pi_u^4 3d\delta_g^1)$
B_2 (B5.5-$s2p2$)	$^3\Sigma_g^-$ [e]	$^3\Sigma_g^-$ $(2s\sigma_g^2 2s\sigma_u^2 2\pi_u^2)$	V_2 (V7.5-$s2p2d2$)	$^3\Sigma_g^-$ [n]	$^1\Sigma_g^+$ $(4s\sigma_g^2 3d\sigma_g^2 3d\pi_u^4 3d\delta_g^2)$
C_2 (C5.0-$s2p2$)	$^1\Sigma_g^+$ [f]	$^1\Sigma_g^+$ $(2s\sigma_g^2 2s\sigma_u^2 2p\pi_u^4)$	V_2 (V7.5-$s4p4d4f2$)	$^3\Sigma_g^-$ [n]	$^3\Sigma_g^-$ $(4s\sigma_g^2 3d\sigma_g^2 3d\pi_u^4 3d\delta_g^2)$
N_2 (N5.0-$s2p2$)	$^1\Sigma_g^+$ [f]	$^1\Sigma_g^+$ $(2s\sigma_u^2 2p\pi_u^4 2p\sigma_g^2)$	Cr_2 (Cr7.0-$s2p2d2$)	$^1\Sigma_g^+$ [o]	$^1\Sigma_g^+$ $(4s\sigma_g^2 3d\sigma_g^2 3d\pi_u^4 3d\delta_g^4)$
O_2 (O5.0-$s2p2$)	$^3\Sigma_g^-$ [f]	$^3\Sigma_g^-$ $(2p\sigma_g^2 2p\pi_u^4 2p\pi_g^2)$	MnO (Mn7.0-$s2p2d2$)	$^6\Sigma^+$ [p]	$^6\Sigma^+$ $(d\sigma^1 d\pi^4 d\delta^2 d\pi^{*2})$
F_2 (F5.0-$s2p2$)	$^1\Sigma_g^+$ [f]	$^1\Sigma_g^+$ $(2p\sigma_g^2 2p\pi_u^4 2p\pi_g^4)$	Fe_2 (Fe7.0-$s2p2d2$)	$^7\Delta_u$ [q]	$^7\Delta_u$ $(4s\sigma_g^2 3d\sigma_g^2 3d\sigma_u^1 3d\pi_u^4 3d\pi_g^2 3d\delta_g^3 3d\delta_u^2)$
Ne_2 (Ne7.0-$s2p2$)	$^1\Sigma_g^+$ [g]	$^1\Sigma_g^+$ $(2p\pi_u^4 2p\pi_g^4 2p\sigma_u^2)$	Co_2 (Co7.0-$s2p2d2$)		$^5\Delta_g$ $(4s\sigma_g^2 3d\sigma_g^2 3d\sigma_u^1 3d\pi_u^4 3d\pi_g^2 3d\delta_g^4 3d\delta_u^3)$
Na_2 (Na9.0-$s2p2$)	$^1\Sigma_g^+$ [f]	$^1\Sigma_g^+$ $(2p\pi_g^4 2p\sigma_u^2 3s\sigma_g^2)$	Ni_2 (Ni7.0-$s2p2d2$)	Ω [r]	$^3\Sigma_g^-$ $(4s\sigma_g^2 3d\sigma_g^2 3d\sigma_u^2 3d\pi_u^4 3d\pi_g^2 3d\delta_g^4 3d\delta_u^4)$
MgO (Mg7.0-$s2p2$)	$^1\Sigma^+$ [h]	$^1\Sigma^+$ $(s\sigma^2 s\sigma^2 p\pi^4)$	Cu_2 (Cu7.0-$s2p2d2$)	$^1\Sigma_g^+$ [s]	$^1\Sigma_g^+$ $(4s\sigma_g^2 3d\sigma_g^2 3d\sigma_u^2 3d\pi_u^4 3d\pi_g^4 3d\delta_g^4 3d\delta_u^4)$
Al_2 (Al6.5-$s2p2$)	$^3\Pi_u$ [i]	$^3\Sigma_g^-$ $(3s\sigma_g^2 3s\sigma_u^2 3p\pi_u^2)$	ZnH (Zn7.0-$s2p2d2$)	$^2\Sigma_g^+$ [t]	$^2\Sigma_g^+$ $(s\sigma^2 s\sigma^{*1} d\sigma^2 d\pi^4 d\delta^4)$
Al_2 (Al6.5-$s4p4d2$)	$^3\Pi_u$ [i]	$^3\Sigma_g^-$ $(3s\sigma_g^2 3s\sigma_u^2 3p\pi_u^2)$	GaH (Ga7.0-$s2p2$)	$^1\Sigma^+$ [u]	$^1\Sigma^+$ $(s\sigma^2 s\sigma^{*2})$
Si_2 (Si6.5-$s2p2$)	$^3\Sigma_g^-$ [f]	$^3\Pi_u$ $(3s\sigma_u^2 3s\sigma_g^1 3p\pi_u^3)$	GeO (Ge7.0-$s2p2$)	$^1\Sigma^+$ [f]	$^1\Sigma^+$ $(ss\sigma^2 sp\sigma^2 pp\pi^4 pp\sigma^2)$
Si_2 (Si6.5-$s2p2d1$)	$^3\Sigma_g^-$ [f]	$^3\Sigma_g^-$ $(3s\sigma_u^2 3p\pi_u^2 3s\sigma_g^2)$	As_2 (As7.0-$s2p2d1$)	$^1\Sigma_g^+$ [f]	$^1\Sigma_g^+$ $(4s\sigma_g^2 4s\sigma_u^2 4p\sigma_g^2 4p\pi_u^4)$
P_2 (P6.0-$s2p2d1$)	$^1\Sigma_g^+$ [f]	$^1\Sigma_g^+$ $(3s\sigma_u^2 3p\sigma_g^2 3p\pi_u^4)$	Se_2 (Se7.0-$s2p2d1$)	$^3\Sigma_g^-$ [f]	$^3\Sigma_g^-$ $(4s\sigma_g^2 4s\sigma_u^2 4p\sigma_g^2 4p\pi_u^4 4p\pi_g^2)$
S_2 (S6.0-$s2p2$)	$^3\Sigma_g^-$ [f]	$^3\Sigma_g^-$ $(3p\sigma_g^2 3p\pi_u^4 3p\pi_g^2)$	Br_2 (Br7.0-$s2p2d1$)	$^1\Sigma_g^+$ [f]	$^1\Sigma_g^+$ $(4s\sigma_g^2 4s\sigma_u^2 4p\sigma_g^2 4p\pi_u^4 4p\pi_g^4)$
Cl_2 (Cl6.0-$s2p2d2$)	$^1\Sigma_g^+$ [f]	$^1\Sigma_g^+$ $(3p\sigma_g^2 3p\pi_u^4 3p\pi_g^4)$	Kr_2 (Kr7.0-$s2p2$)	$^1\Sigma_g^+$ [v]	$^1\Sigma_g^+$ $(4s\sigma_g^2 4s\sigma_u^2 4p\sigma_g^2 4p\sigma_u^2 4p\pi_u^4 4p\pi_g^4)$
Ar_2 (Ar7.0-$s2p2$)	$^1\Sigma_g^+$ [j]	$^1\Sigma_g^+$ $(3p\pi_u^4 3p\pi_g^4 3p\sigma_u^2)$			

All the successes and failures by the LDA are reproduced by the modest size of basis functions (DNP in most cases)

Variational optimization of basis functions

One-particle wave functions

$$\psi_\mu(\mathbf{r}) = \sum_{i\alpha} c_{\mu,i\alpha}\phi_{i\alpha}(\mathbf{r}-\mathbf{r}_i)$$

Contracted orbitals

$$\phi_{i\alpha}(\mathbf{r}) = \sum_q a_{i\alpha q}\chi_{i\eta}(\mathbf{r})$$

The variation of E with respect to *c* with fixed *a* gives

$$\partial E_{\mathrm{tot}}/\partial c_{\mu,i\alpha} = 0 \quad \rightarrow \quad \sum_{j\beta} \langle \phi_{i\alpha}|\hat{H}|\phi_{j\beta}\rangle c_{\mu,j\beta} = \varepsilon_\mu \sum_{j\beta} \langle \phi_{i\alpha}|\phi_{j\beta}\rangle c_{\mu,j\beta}$$

Regarding c as dependent variables on *a* and assuming KS eq. is solved self-consistently with respect to *c*, we have

$$\frac{\partial E_{\mathrm{tot}}}{\partial a_{i\alpha q}} = \frac{\delta E_{\mathrm{tot}}}{\delta \rho(\mathbf{r})}\frac{\delta \rho(\mathbf{r})}{\delta a_{i\alpha q}}$$

$$= 2\sum_{j\beta} \left(\Theta_{i\alpha,j\beta}\langle \chi_{i\eta}|\hat{H}|\phi_{j\beta}\rangle - E_{i\alpha,j\beta}\langle \chi_{i\eta}|\phi_{j\beta}\rangle\right)$$

Ozaki, PRB 67, 155108 (2003)

Optimization of basis functions

1. Choose typical chemical environments


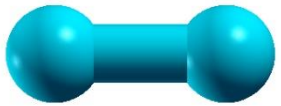


2. Optimize variationally the radial functions

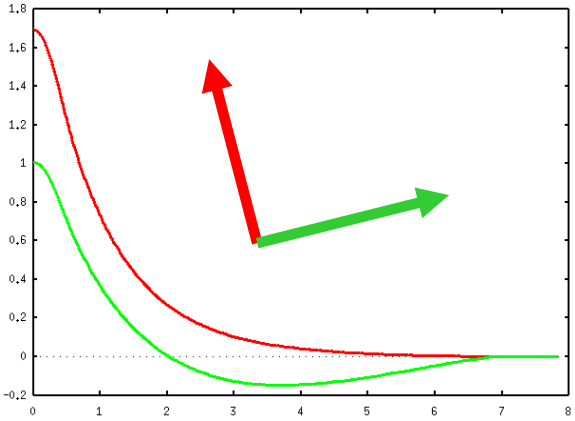
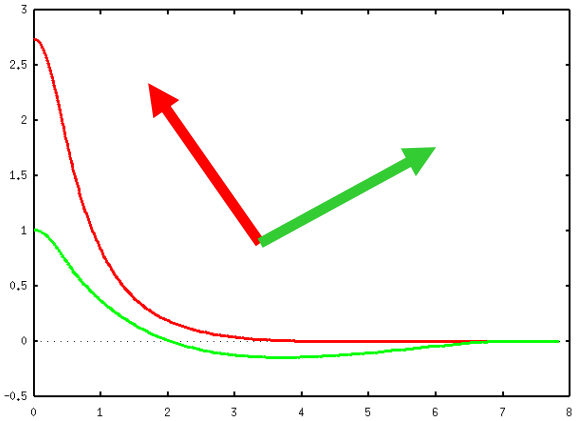
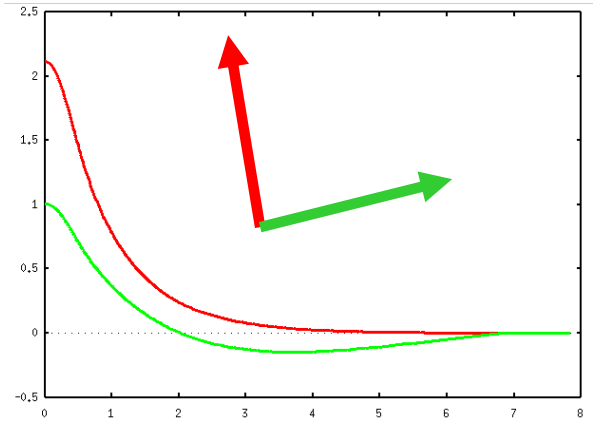

3. Rotate a set of optimized orbitals within the subspace, and discard the redundant funtions

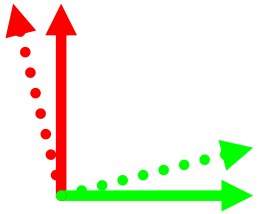
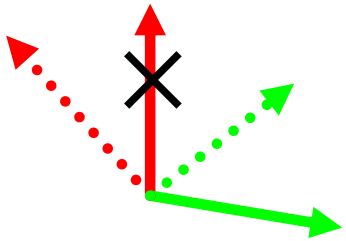
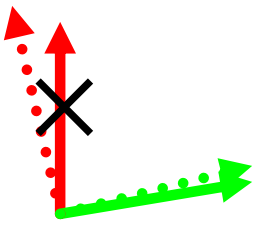

Database of optimized VPS and PAO

Database (2013) of optimized VPS and PAO

The database (2013) of fully relativistic pseudopotentials (VPS) and pseudo-atomic orbitals (PAO), generated by ADPACK, which could be an input data of program package, OpenMX. The data of elements with the underline are currently available. When you use these data, VPS and PAO, in the program package, OpenMX, then copy them to the directory, openmx*.*/DFT_DATA13/VPS/ and openmx*.*/DFT_DATA13/PAO/, respectively. The delta factor of OpenMX with the database (2013) is found at here.

E																	
H																	He
Li	Be											B	C	N	O	F	Ne
Na	Mg											Al	Si	P	S	Cl	Ar
K	Ca	Sc	Ti	V	Cr	Mn	Fe	Co	Ni	Cu	Zn	Ga	Ge	As	Se	Br	Kr
Rb	Sr	Y	Zr	Nb	Mo	Tc	Ru	Rh	Pd	Ag	Cd	In	Sn	Sb	Te	I	Xe
Cs	Ba	L	Hf	Ta	W	Re	Os	Ir	Pt	Au	Hg	Tl	Pb	Bi	Po	At	Rn
Fr	Ra	A															
	L	La	Ce	Pr	Nd	Pm	Sm	Eu	Gd	Tb	Dy	Ho	Er	Tm	Yb	Lu	
	A	Ac	Th	Pa	U	Np	Pu	Am	Cm	Bk	Cf	Es	Fm	Md	No	Lr	

Public release of optimized and well tested VPS and PAO so that users can easily start their calculations.

Reproducibility in DFT calcs

RESEARCH ARTICLE

Science 351, aad3000 (2016)

DFT METHODS

Reproducibility in density functional theory calculations of solids

Kurt Lejaeghere,[1*] Gustav Bihlmayer,[2] Torbjörn Björkman,[3,4] Peter Blaha,[5] Stefan Blügel,[2] Volker Blum,[6] Damien Caliste,[7,8] Ivano E. Castelli,[9] Stewart J. Clark,[10] Andrea Dal Corso,[11] Stefano de Gironcoli,[11] Thierry Deutsch,[7,8] John Kay Dewhurst,[12] Igor Di Marco,[13] Claudia Draxl,[14,15] Marcin Dułak,[16] Olle Eriksson,[13] José A. Flores-Livas,[12] Kevin F. Garrity,[17] Luigi Genovese,[7,8] Paolo Giannozzi,[18] Matteo Giantomassi,[19] Stefan Goedecker,[20] Xavier Gonze,[19] Oscar Grånäs,[13,21] E. K. U. Gross,[12] Andris Gulans,[14,15] François Gygi,[22] D. R. Hamann,[23,24] Phil J. Hasnip,[25] N. A. W. Holzwarth,[26] Diana Iuşan,[13] Dominik B. Jochym,[27] François Jollet,[28] Daniel Jones,[29] Georg Kresse,[30] Klaus Koepernik,[31,32] Emine Küçükbenli,[9,11] Yaroslav O. Kvashnin,[13] Inka L. M. Locht,[13,33] Sven Lubeck,[14] Martijn Marsman,[30] Nicola Marzari,[9] Ulrike Nitzsche,[31] Lars Nordström,[13] Taisuke Ozaki,[34] Lorenzo Paulatto,[35] Chris J. Pickard,[36] Ward Poelmans,[1,37] Matt I. J. Probert,[25] Keith Refson,[38,39] Manuel Richter,[31,32] Gian-Marco Rignanese,[19] Santanu Saha,[20] Matthias Scheffler,[15,40] Martin Schlipf,[22] Karlheinz Schwarz,[5] Sangeeta Sharma,[12] Francesca Tavazza,[17] Patrik Thunström,[41] Alexandre Tkatchenko,[15,42] Marc Torrent,[28] David Vanderbilt,[23] Michiel J. van Setten,[19] Veronique Van Speybroeck,[1] John M. Wills,[43] Jonathan R. Yates,[29] Guo-Xu Zhang,[44] Stefaan Cottenier[1,45*]

15 codes
69 researchers
71 elemental bulks
GGA-PBE
Scalar relativistic

PBE lattice constant of Si

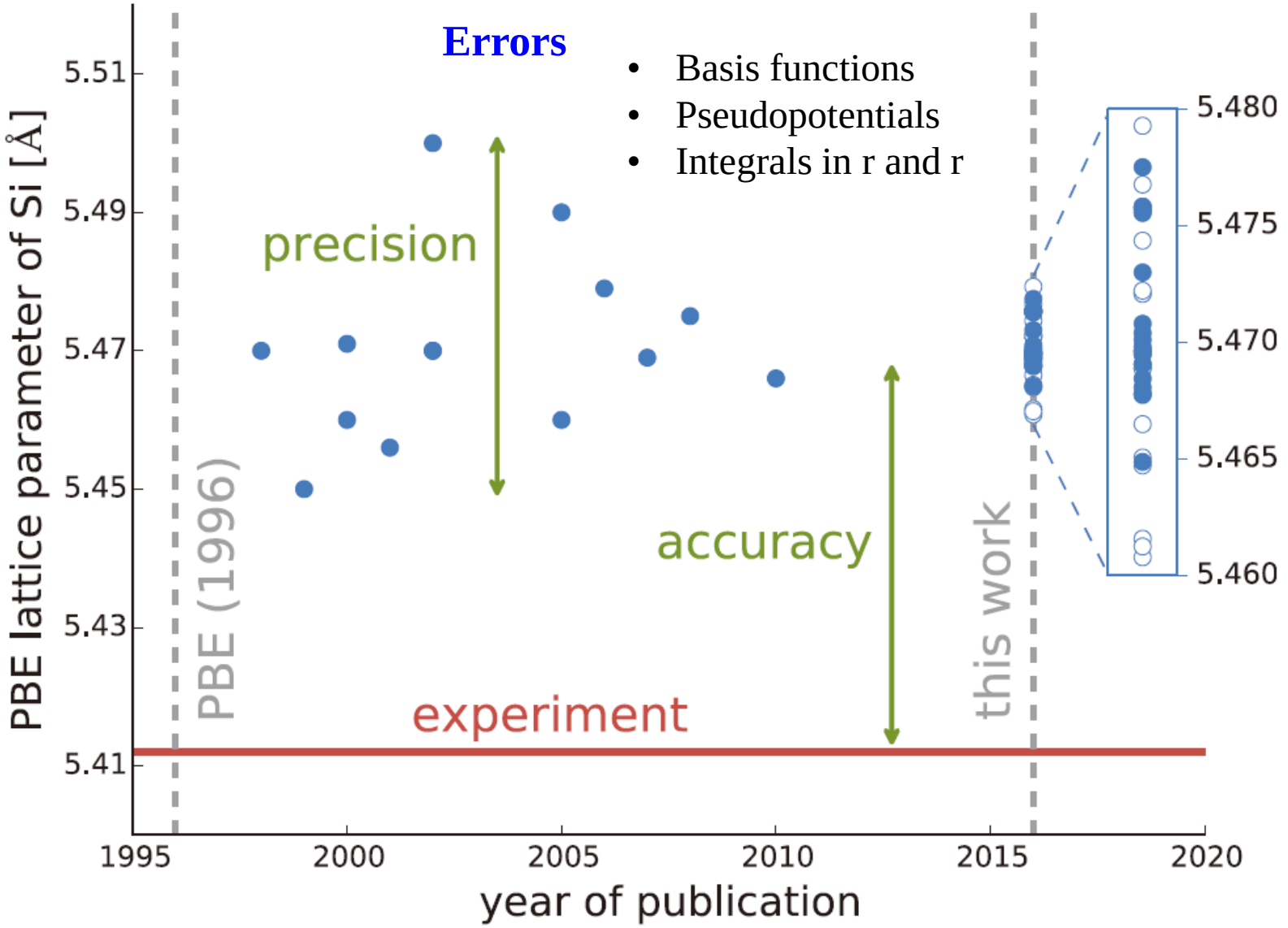

Δ-gauge

A way of comparing accuracy of codes

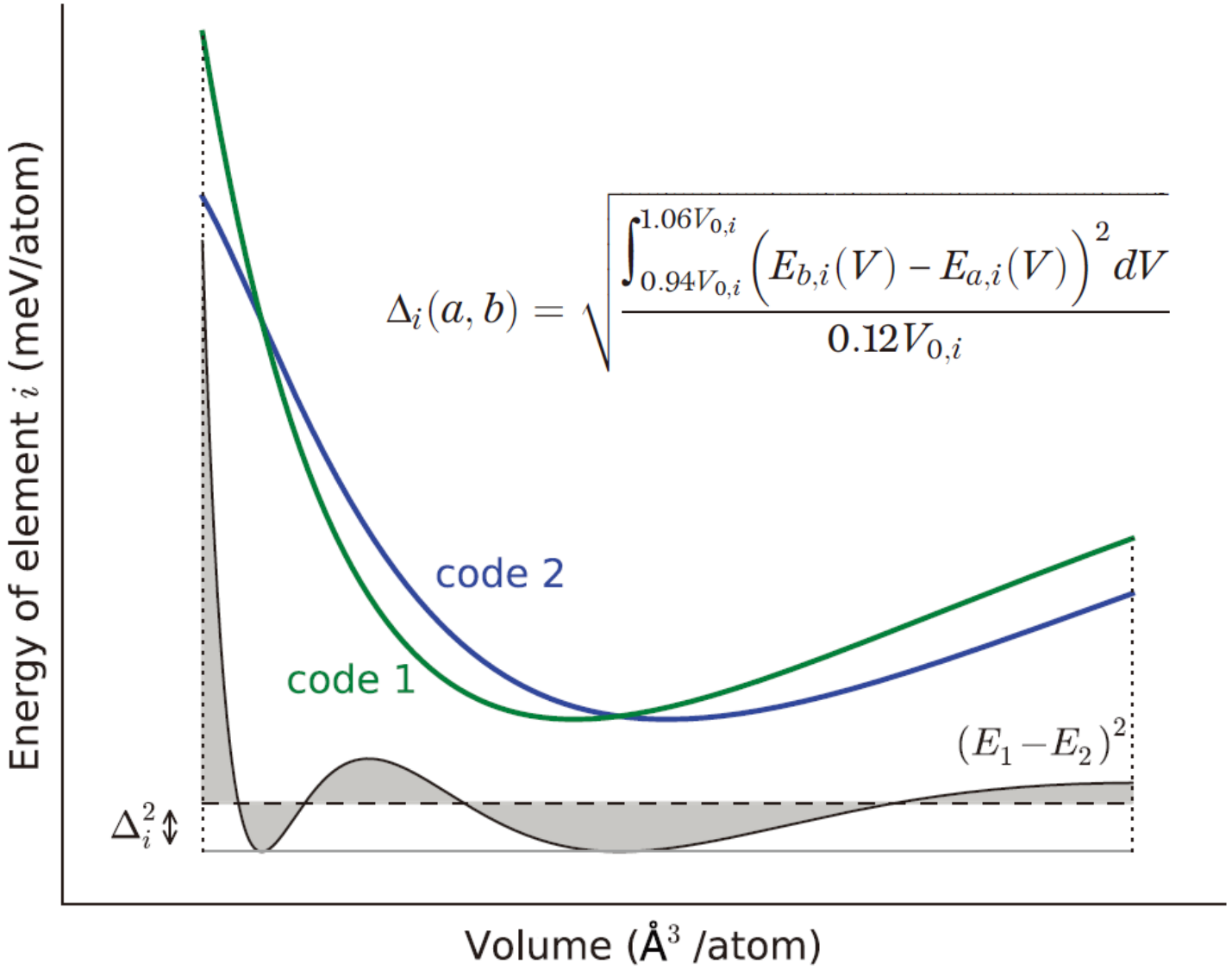

Evaluation of GGA-PBE By Δ-gauge

In comparison of GGA-PBE with Expts. of 58 elements, the mean Δ-gauge is 23.5meV/atom.

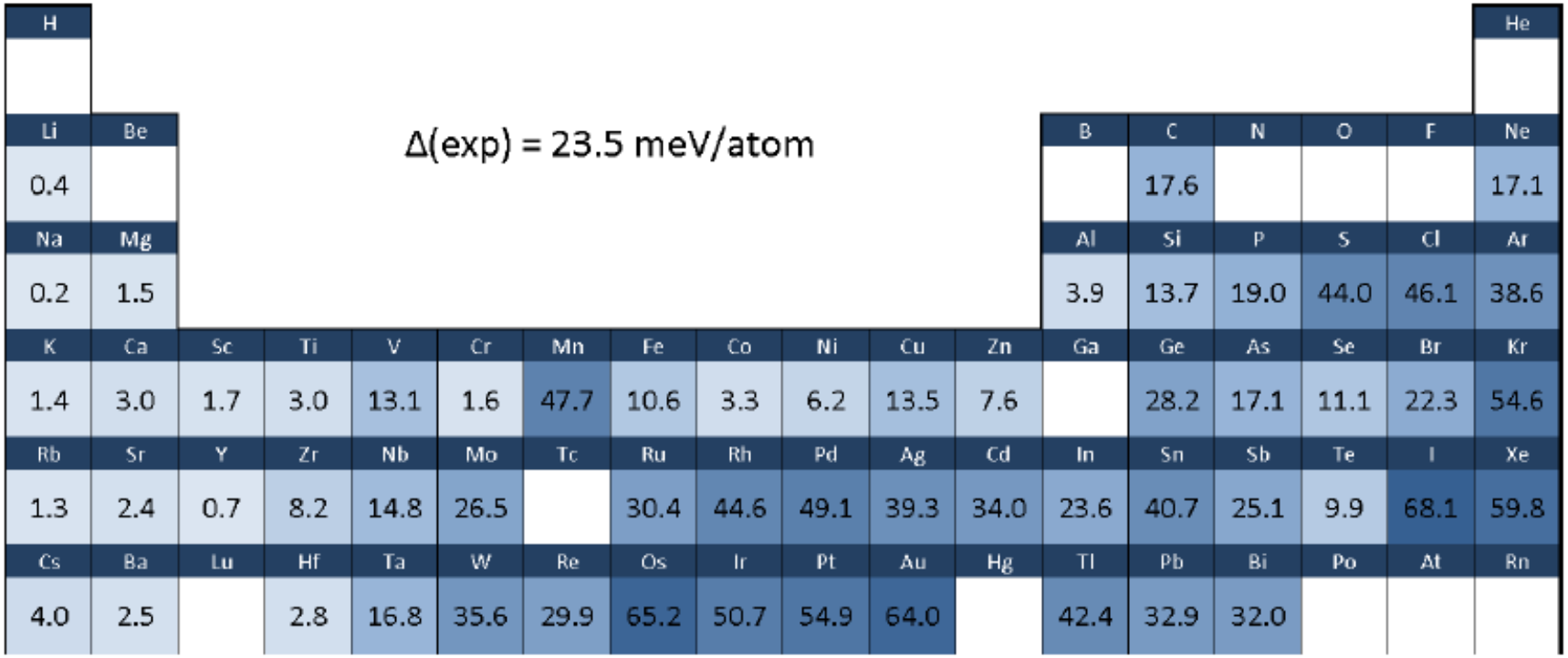

Comparison of codes by Δ-gauge

Type	Code	average <Δ>	Elk	exciting	FHI-aims/tier2	FLEUR	FPLO/T+F+s	RSPt	WIEN2k/acc
NCPP	ONCVPSP(SG15)2/CASTEP	1.4	1.4	1.4	1.4	1.3	1.6	1.5	1.4
	ONCVPSP(SG15)1/QE	1.4	1.4	1.3	1.3	1.3	1.6	1.5	1.3
	ONCVPSP(PD0.1)/ABINIT	0.7	0.7	0.7	0.7	0.6	1.0	0.8	0.6
	MBK2013/OpenMX	2.0	2.1	2.1	2.1	1.9	1.8	1.8	2.0
	HGH-NLCC/BigDFT	1.1	1.1	1.1	1.1	1.0	1.2	1.1	1.0
	HGH/ABINIT	2.2	2.2	2.2	2.2	2.0	2.3	2.2	2.1
	FHI98pp/ABINIT	13.3	13.5	13.4	13.4	13.2	13.0	13.2	13.4
USPP	Vdb2/DACAPO	6.3	6.3	6.3	6.3	6.3	6.4	6.5	6.2
	SSSP/QE	0.5	0.4	0.3	0.3	0.5	0.9	0.8	0.3
	OTFG9/CASTEP	0.7	0.4	0.5	0.5	0.7	1.0	1.0	0.5
	GBRV14/QE	1.1	1.0	1.0	0.9	1.0	1.4	1.3	1.0
	GBRV14/CASTEP	1.1	1.1	1.1	1.0	1.0	1.4	1.3	1.0
PAW	VASPGW2015/VASP	0.6	0.4	0.4	0.4	0.6	1.0	0.8	0.3
	PSlib100/QE	0.9	0.9	0.8	0.8	0.8	1.3	1.1	0.8
	JTH02/ABINIT	0.6	0.6	0.6	0.6	0.6	0.9	0.7	0.5
	GPAW09/GPAW	1.6	1.5	1.5	1.5	1.5	1.8	1.7	1.5
	GPAW09/ABINIT	1.4	1.3	1.3	1.3	1.3	1.7	1.5	1.3
	GBRV12/ABINIT	0.9	0.9	0.8	0.8	0.9	1.3	1.1	0.8
AE	WIEN2k/acc	0.5	0.3	0.2	0.2	0.4	0.9	0.8	
	RSPt	0.8	0.9	0.8	0.8	0.6	0.9		0.8
	FPLO/T+F+s	0.9	1.0	0.9	0.9	0.8		0.9	0.9
	FLEUR	0.6	0.6	0.5	0.5		0.8	0.6	0.4
	FHI-aims/tier2	0.5	0.3	0.1		0.5	0.9	0.8	0.2
	exciting	0.5	0.3		0.1	0.5	0.9	0.8	0.2
	Elk	0.6		0.3	0.3	0.6	1.0	0.9	0.3

The mean Δ-gauge of OpenMX is 2.0meV/atom.

Practical guide to OpenMX calculations

- Choice of cutoff energy
- Calculations of energy curves
- SCF calculations
- How to choose basis functions
- Work functions and floating states
- Overcompleteness
- Restarting
- Outputting in a binary mode

Choice of cutoff energy

scf.energycutoff 200 # default=150 Ryd

The FFT grid is used to discretize real space and calculate $E_{\delta ee}$, E_{xc}, and can be specified by scf.energycutoff.

In most cases, 200 Ryd is enough to get convergence.

However, large cutoff energy (300-400 Ryd) has be used for cases such as use of pseudopotentials with deep semi-core states.

Memory requiment
$O(E^{3/2})$

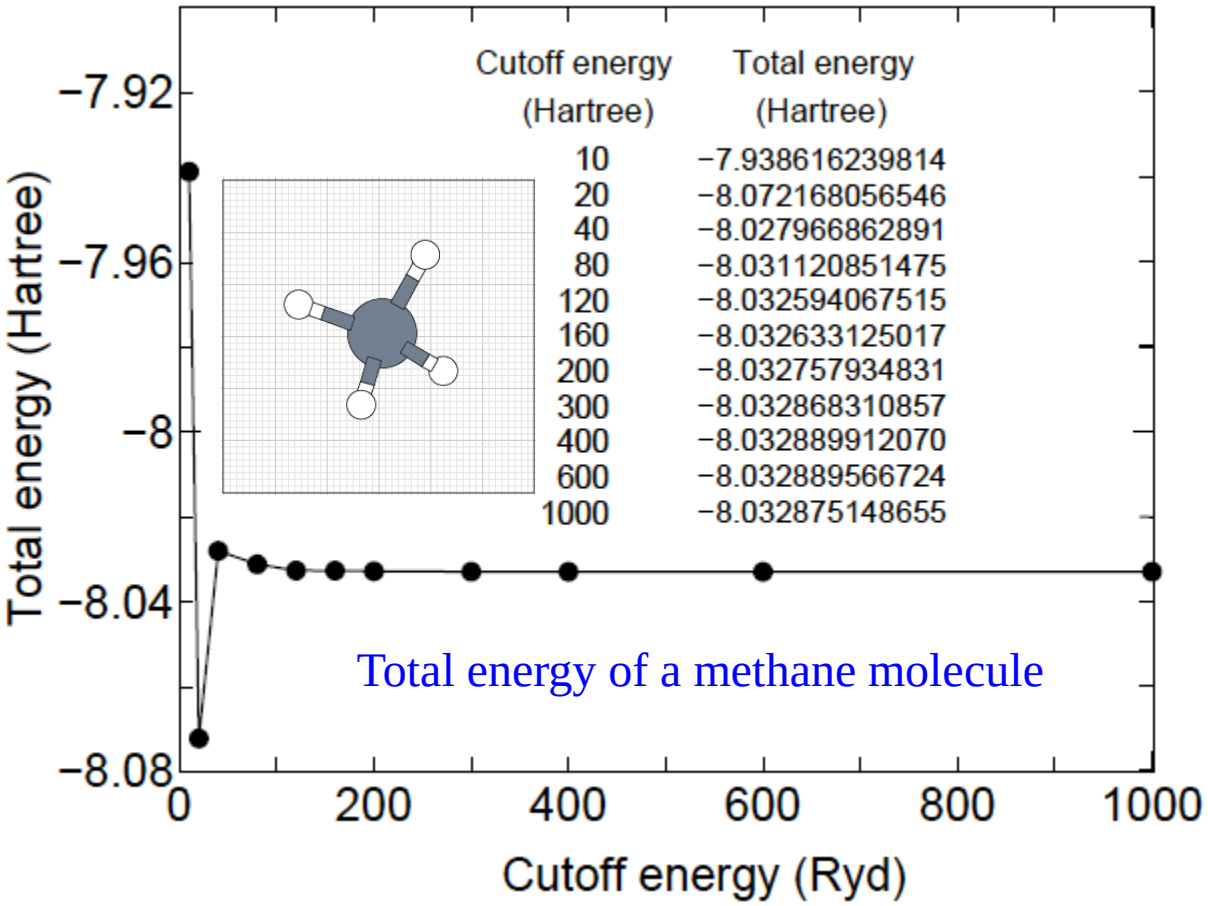

Choice of cutoff energy

Geometry optimization of H_2O

Dependency of optimized structure of H_2O on scf.energycutoff. It turns out that 180Ryd. is enough to reach the convergence.

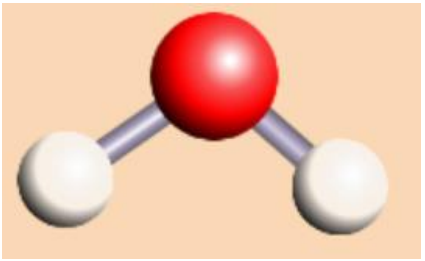

Table 1: Convergence of structural parameters, dipole moment of a water molecule with respect to the cutoff energy. The input file is 'H2O.dat' in the directory 'work'.

Ecut(Ryd)	r(H-O) (Å)	∠ (H-O-H) (deg)	Dipole moment (Debye)
60	0.970	103.4	1.838
90	0.971	103.7	1.829
120	0.971	103.7	1.832
150	0.971	103.6	1.829
180	0.971	103.6	1.833
Exp.	0.957	104.5	1.85

Volume vs. Energy curves

The following keywords are available to calculate energy curves.

```
MD.Type          EvsLC    #
MD.EvsLC.Step    0.4      # default=0.4%
MD.maxIter       32       # default=1
```

When the energy curve for bulk system is calculated as a function of the lattice parameter, a sudden change of the number of real space grids is a serious problem which produces an erratic discontinuity on the energy curve. To avoid this, the number of grids should be fixed by explicitly specifying the following keyword:

```
scf.Ngrid        32 32 32
```

The numbers correspond to the number of grid along a-, b-, and c-axes, respectively. scf.Ngrid is used if both the keywords scf.energycutoff and scf.Ngrid are specified.

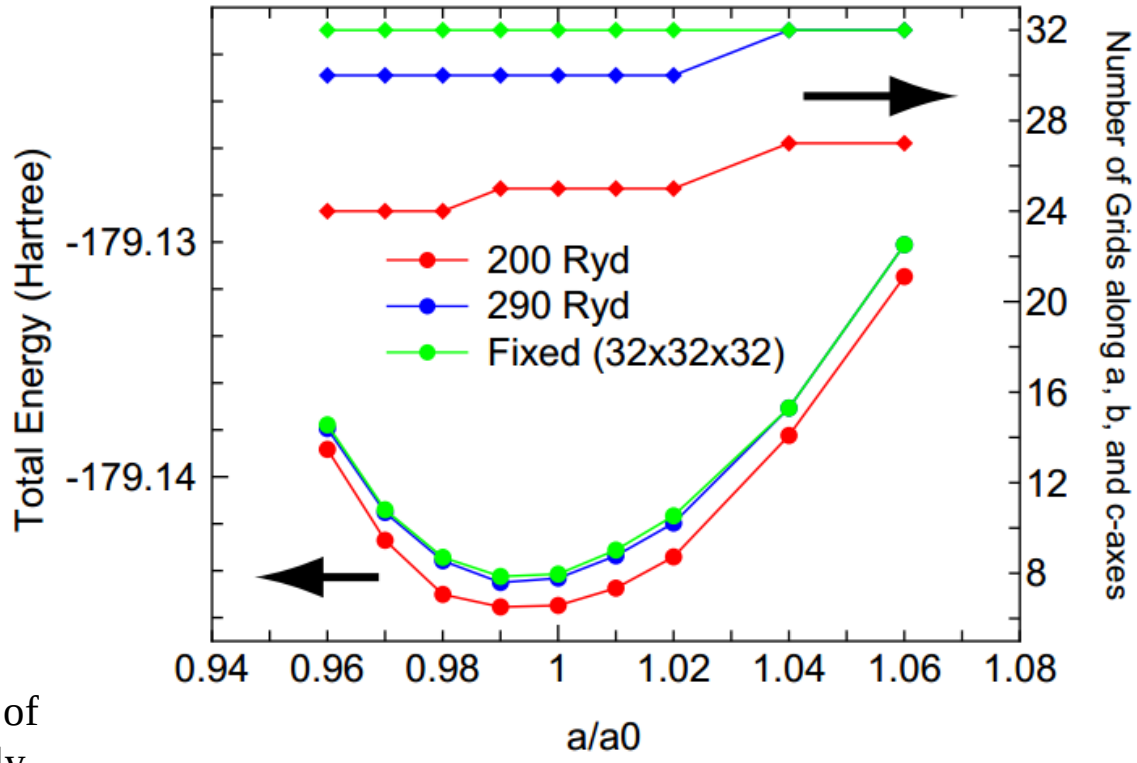


```
MD.EvsLC.flag    1  1  0      # along a, b, c-axes
1: varied,  0: fixed
```

Self-consistency: Simple charge mixing

The KS effective is constructed from ρ.
However, ρ is evaluated from eigenfaunctions of KS eq.

$$\hat{H}_{\mathrm{KS}}\phi_i = \varepsilon_i\phi_i \qquad \hat{H}_{\mathrm{KS}} = -\frac{1}{2}\nabla^2 + v_{\mathrm{eff}}$$

$$v_{\mathrm{eff}} = v_{\mathrm{ext}}(\mathbf{r}) + v_{\mathrm{Hartree}}(\mathbf{r}) + \frac{\delta E_{\mathrm{xc}}}{\delta\rho(\mathbf{r})}$$

$$\rho(\mathbf{r}) = \sum_i \phi_i^*(\mathbf{r})\phi_i(\mathbf{r})$$

Simple charge mixing method

The next input density is constructed by a simple mixing of input and output densities.

$$\rho_{n+1}^{(\mathrm{in})} = \alpha\rho_n^{(\mathrm{in})} + (1-\alpha)\rho_n^{(\mathrm{out})},$$

It works well for large gap systems and small sized systems.

Self-consistency: RMM-DIIS

Idea:

Minimize the norm of a linear combination of previous residual vectors.

$$\bar{R}_{n+1} = \sum_{m=n-(p-1)}^{n} \alpha_m R_m,$$

$$\begin{aligned} F &= \langle \bar{R}_{n+1} | \bar{R}_{n+1} \rangle - \lambda \left(1 - \sum_m^n a_m \right), \\ &= \sum_{m,m'} \alpha_m \alpha_{m'} \langle R_m | R_{m'} \rangle - \lambda \left(1 - \sum_m^n a_m \right). \end{aligned}$$

$$R_n(\mathbf{q}) \equiv \tilde{n}_n^{(\mathrm{out})}(\mathbf{q}) - \tilde{n}_n^{(\mathrm{in})}(\mathbf{q}),$$

$$\langle R_m | R_{m'} \rangle \equiv \sum_{\mathbf{q}} \frac{R_m^*(\mathbf{q}) R_{m'}(\mathbf{q})}{w(\mathbf{q})},$$

Kerker factor

$$w(\mathbf{q}) = \frac{|\mathbf{q}|^2}{|\mathbf{q}|^2 + q_0^2},$$

Long wave length components corresponding to small |q| are taken into account.

Minimization of F leads to

$$\frac{\partial F}{\partial \alpha_k} = 0 \qquad \frac{\partial F}{\partial \lambda} = 0$$

$$\begin{pmatrix} \langle R_{n-(p-1)} | R_{n-(p-1)} \rangle & \cdots & \cdots & 1 \\ \cdots & \cdots & \cdots & 1 \\ \cdots & \cdots & \langle R_n | R_n \rangle & \cdots \\ 1 & 1 & \cdots & 0 \end{pmatrix} \begin{pmatrix} \alpha_{n-(p-1)} \\ \alpha_{n-(p-1)+1} \\ \cdot \\ \frac{1}{2}\lambda \end{pmatrix} = \begin{pmatrix} 0 \\ 0 \\ \cdot \\ 1 \end{pmatrix}.$$

Optimum input density might be given by

$$\rho_{n+1}^{(\mathrm{in})} = \sum_{m=n-(p-1)}^{n} \alpha_m \rho_m^{(\mathrm{in})} + \beta \sum_{m=n-(p-1)}^{n} \alpha_m R_m$$

G.Kresse and J. Furthmeuller, PRB 54, 11169 (1996).

Mixing methods

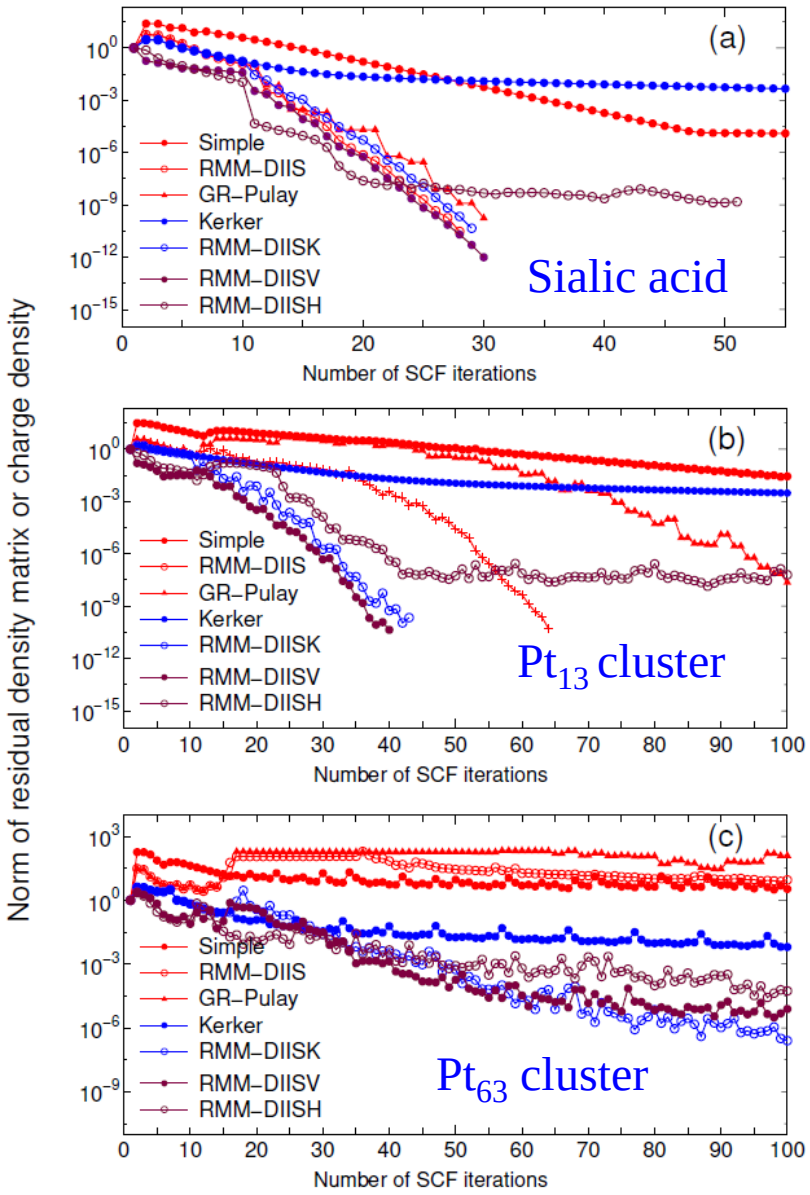

Available mixing methods:

Simple mixing (Simple)

Residual minimization method in the direct inversion iterative subspace (RMM-DIIS)

Guaranteed reduction Pulay method (GR-Pulay)

Kerker mixing (Kerker)

RMM-DIIS with Kerker metric (RMM-DIISK)

RMM-DIIS for Kohn-Sham potential (RMM-DIISV)

RMM-DIIS for Hamiltonian (RMM-DIISH)

Recommendation:
RMM-DIISK or RMM-DIISV

For DFT+U and constrained methods
RMM-DIISH

See also the page 63 in the manual.

Database of PAO and VPS

https://t-ozaki.issp.u-tokyo.ac.jp/vps_pao2019/

Database (2019) of optimized VPS and PAO

The database (2019) of fully relativistic pseudopotentials (VPS) and pseudo-atomic orbitals (PAO), generated by ADPACK, which could be an input data of program package, OpenMX. The data of elements with the underline are currently available. When you use these data, VPS and PAO, in the program package, OpenMX, then copy them to the directory, openmx*.*/DFT_DATA19/VPS/ and openmx*.*/DFT_DATA19/PAO/, respectively. The delta gauge of OpenMX with the database (2019) is found at here.

Public release of optimized and well tested VPS and PAO so that users can easily start their calculations.

E																	
H																	He
Li	Be											B	C	N	O	F	Ne
Na	Mg											Al	Si	P	S	Cl	Ar
K	Ca	Sc	Ti	V	Cr	Mn	Fe	Co	Ni	Cu	Zn	Ga	Ge	As	Se	Br	Kr
Rb	Sr	Y	Zr	Nb	Mo	Tc	Ru	Rh	Pd	Ag	Cd	In	Sn	Sb	Te	I	Xe
Cs	Ba	L	Hf	Ta	W	Re	Os	Ir	Pt	Au	Hg	Tl	Pb	Bi	Po	At	Rn
Fr	Ra	A															
	L	La	Ce	Pr	Nd	Pm	Sm	Eu	Gd	Tb	Dy	Ho	Er	Tm	Yb	Lu	
	A	Ac	Th	Pa	U	Np	Pu	Am	Cm	Bk	Cf	Es	Fm	Md	No	Lr	

Specification of PAO and VPS

PAO and VPS are specified by the following keyword:

```
<Definition.of.Atomic.Species
  O    O7.0-s2p2d1       O_PBE19
  H    H7.0-s2p1         H_PBE19
Definition.of.Atomic.Species>
```

- O7.0 means O7.0.pao.
- -s2p2d1 means 2, 2, and 1 radial functions are allocated to s-, p-, and d-orbitals.
- In this case, for oxygen atom, 2×1+2×3+1×5=13 basis functions are allocated.
- O_PBE19 means O_PBE19.vps.

The path for O7.0.pao and O_PBE19.vps is specified by

DATA.PATH /home/soft/openmx3.9/DFT_DATA19

Default value is '../DFT_DATA19'.

How to choose basis functions: H_2O case

By clicking H7.0.pao and O7.0.pao in the database(2019), you may find the following

https://t-ozaki.issp.u-tokyo.ac.jp/vps_pao2019/H/index.html

H7.0.pao

```
**************************************************
  Eigen values(Hartree) of pseudo atomic orbitals
**************************************************

Eigenvalues
Lmax= 3 Mul=15
  | mu    0  0     -0.23595211038442   <- 3
  | mu    0  1      0.14109389991827   <- 6
  | mu    0  2      0.61751730037441
  | mu    0  3      1.31890671598573
  | mu    0  4      2.24052765608302
  | mu    0  5      3.37954791544661
  | mu    0  6      4.73488369825610
  | mu    0  7      6.30608874470710
  | mu    0  8      8.09282718517299
  | mu    0  9     10.09464035732420
  | mu    0 10     12.31085267019158
  | mu    0 11     14.74057314485273
  | mu    0 12     17.38277845742691
  | mu    0 13     20.23645090753857
  | mu    0 14     23.30073926597344   <- 5
  | mu    1  0      0.10914684890465
  | mu    1  1      0.47776040452236
  | mu    1  2      1.06988680483686
  | mu    1  3      1.88261331124981
  | mu    1  4      2.91175885838084
  | mu    1  5      4.15601184789448
  | mu    1  6      5.61454131060210
  | mu    1  7      7.28681796296307
  | mu    1  8      9.17254361476158
  | mu    1  9     11.27156766390586
  | mu    1 10     13.58381334569800
  | mu    1 11     16.10921637499960
  | mu    1 12     18.84767560575107
  | mu    1 13     21.79902110024685
  | mu    1 14     24.96300480798286
  | mu    2  0      0.27851528500170
  | mu    2  1      0.76970400958463
  | mu    2  2      1.47576814497054
  | mu    2  3      2.39881523735167
  | mu    2  4      3.53713346447754
```

https://t-ozaki.issp.u-tokyo.ac.jp/vps_pao2019/O/index.html

O7.0.pao

```
**************************************************
  Eigen values(Hartree) of pseudo atomic orbitals
**************************************************

Eigenvalues
Lmax= 3 Mul=15
  | mu    0  0     -0.87913976280231   <- 1
  | mu    0  1      0.06809061901229   <- 4
  | mu    0  2      0.52709275865941
  | mu    0  3      1.24995140722317
  | mu    0  4      2.21829552402723
  | mu    0  5      3.41945468859267
  | mu    0  6      4.84509607059749
  | mu    0  7      6.48825090142865
  | mu    0  8      8.34207134316001
  | mu    0  9     10.39973244132192
  | mu    0 10     12.65513764955926
  | mu    0 11     15.10428688136984
  | mu    0 12     17.74677530362947
  | mu    0 13     20.58633940582683
  | mu    0 14     23.62957122674031   <- 2
  | mu    1  0     -0.33075182895384
  | mu    1  1      0.16376499567753   <- 7
  | mu    1  2      0.64129274864838
  | mu    1  3      1.35995471521821
  | mu    1  4      2.31377697411480
  | mu    1  5      3.50052618379026
  | mu    1  6      4.91841590421346
  | mu    1  7      6.56499793348396
  | mu    1  8      8.43634105410091
  | mu    1  9     10.52733540479795
  | mu    1 10     12.83276989780839
  | mu    1 11     15.34880171573570
  | mu    1 12     18.07414632417004
  | mu    1 13     21.01013110934429
  | mu    1 14     24.15933607166566   <- 8
  | mu    2  0      0.26162948257116
  | mu    2  1      0.70705247436937
  | mu    2  2      1.34714706672243
  | mu    2  3      2.19799459356269
  | mu    2  4      3.26511989658328
```

Choosing states with lower eigenvalues leads to H7.0-s2p1 and O7.0-s2p2d1.

How to choose basis functions: Si case(1)

Si7.0.pao

```
Eigenvalues
Lmax= 3 Mul=15
 | mu    0  0     -0.59320968623145 1
 | mu    0  1      0.01654247265872 4
 | mu    0  2      0.57915688461708 8
 | mu    0  3      1.39915528592998
 | mu    0  4      2.43106703909053
 | mu    0  5      3.63498884739274
 | mu    0  6      4.99885012002783
 | mu    0  7      6.55485759476897
 | mu    0  8      8.33541526908920
 | mu    0  9     10.34055461939939
 | mu    0 10     12.55818051232040
 | mu    0 11     14.98369777887096
 | mu    0 12     17.62014479571136
 | mu    0 13     20.47011746372617
 | mu    0 14     23.53245309073866
 | mu    1  0     -0.31460013133101 2
 | mu    1  1      0.12937640798489 5
 | mu    1  2      0.71637380083701
 | mu    1  3      1.54488697995006
 | mu    1  4      2.59211686526084
 | mu    1  5      3.84687324239366
 | mu    1  6      5.31246180826158
 | mu    1  7      6.99509799702661
 | mu    1  8      8.89454075291723
 | mu    1  9     11.00602102880752
 | mu    1 10     13.32692005826443
 | mu    1 11     15.85857455673626
 | mu    1 12     18.60272353142246
 | mu    1 13     21.55894843635971
 | mu    1 14     24.72602323954447
 | mu    2  0      0.01886411574821 3
 | mu    2  1      0.35893514996065 7
 | mu    2  2      0.94629918754692
 | mu    2  3      1.76201765644983
 | mu    2  4      2.81418723624388
 | mu    2  5      4.10656012645961
 | mu    2  6      5.63661971875011
 | mu    2  7      7.39522693820483
 | mu    2  8      9.37222098331867
 | mu    2  9     11.56227937764802
 | mu    2 10     13.96620568880690
 | mu    2 11     16.58651812641581
 | mu    2 12     19.42296574188659
 | mu    2 13     22.47308081363278
 | mu    2 14     25.73538272482773
 | mu    3  0      0.28356769151846 6
 | mu    3  1      0.79082836114569
 | mu    3  2      1.52992065308726
 | mu    3  3      2.52537261496132
```

Orbitals with lower eigenvalues in Si7.0.pao are taken into account step by step as the quality of basis set is improved.

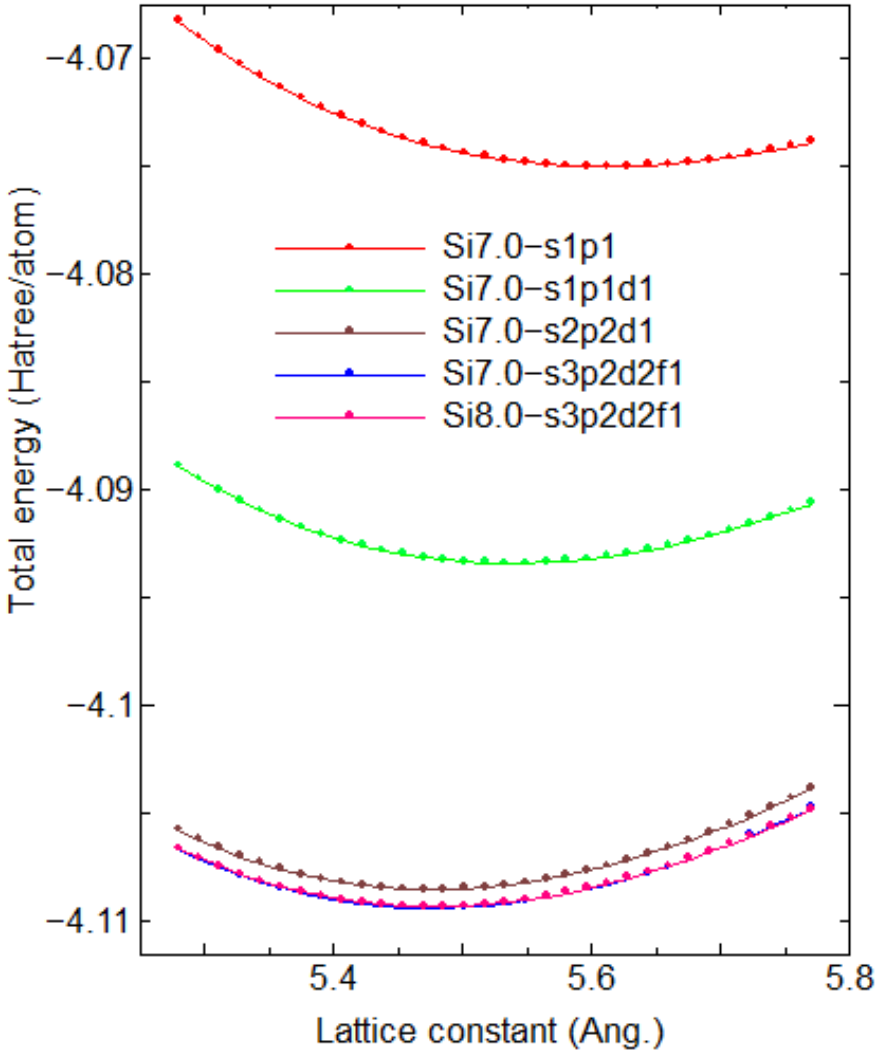

Si7.0-s2p2d1 is enough to discuss structural properties.

By comparing Si7.0-s3p2d2f1 with Si8.0-s3p2d2f1, it turns out that convergence is achieved at the cutoff of 7.0(a.u.).

How to choose basis functions: Si case(2)

With respect to band structure, one can confirm that Si7.0-s2p2d1 provides a nearly convent result.

https://t-ozaki.issp.u-tokyo.ac.jp/vps_pao2019/Si/index.html

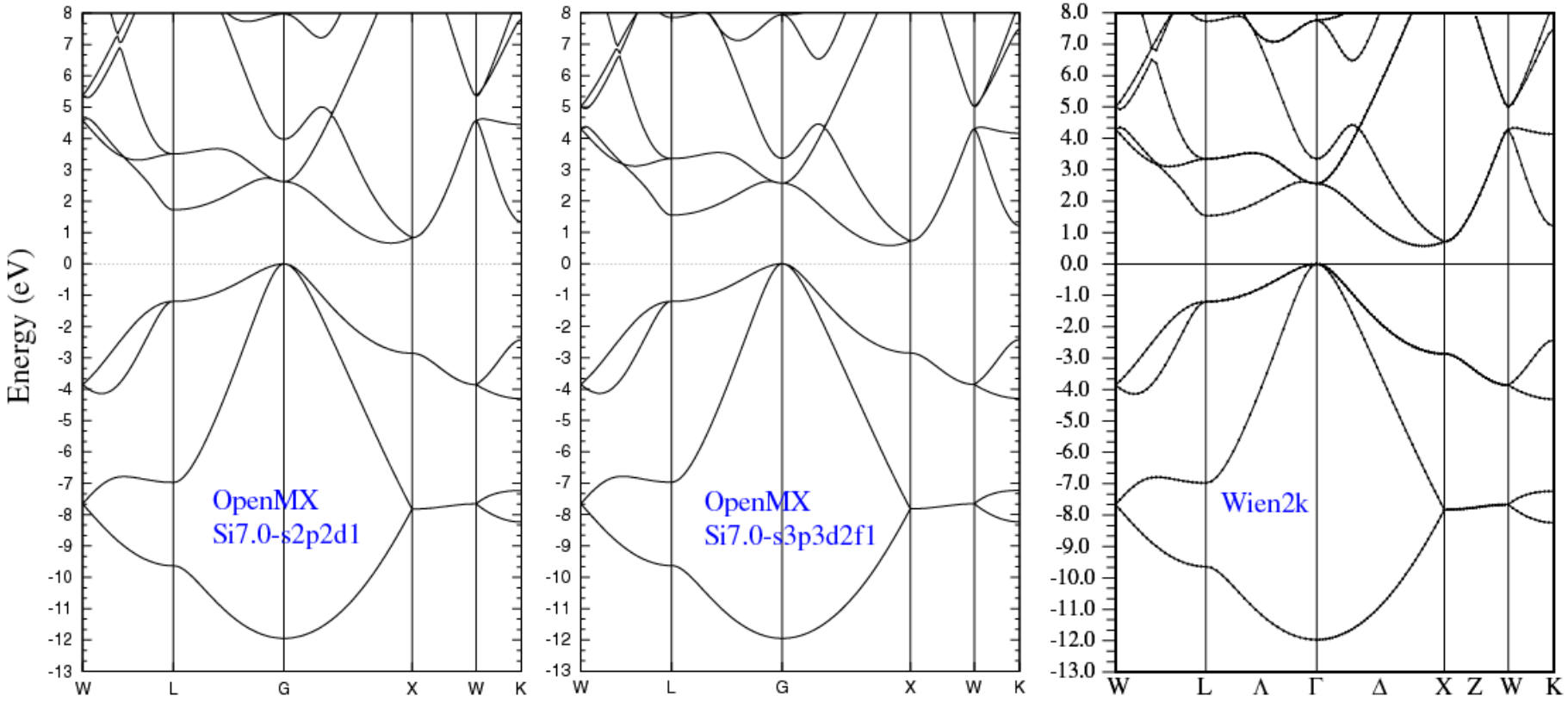

While the convergent result is achieved by use of Si7.0-s3p2d2f1(Si7.0-s3p3d2f1), Si7.0-s2p2d1 is a balanced basis functions compromising accuracy and efficiency to perform a vast range of materials exploration.

Floating states in 3C-SiC

C6.0-s2p2
Si8.0-s2p2

C6.0-s2p2d1
Si8.0-s2p2d1

C6.0-s3p3d2f1
Si8.0-s3p3d2f1

Wien2k (FLAPW)

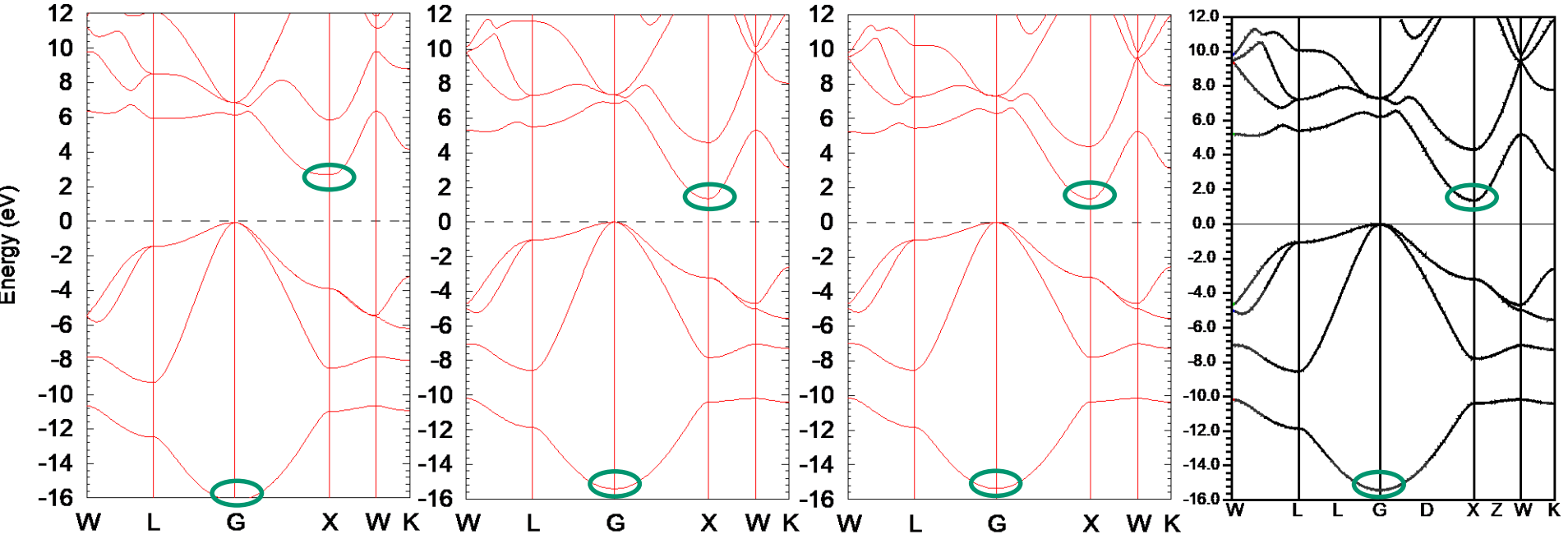

- Inclusion of polarization orbitals is important to reproduce band structures.
- The band structure up to 5 eV is reproduced by s2p2d1.

Basis set superposition Error (BSSE)

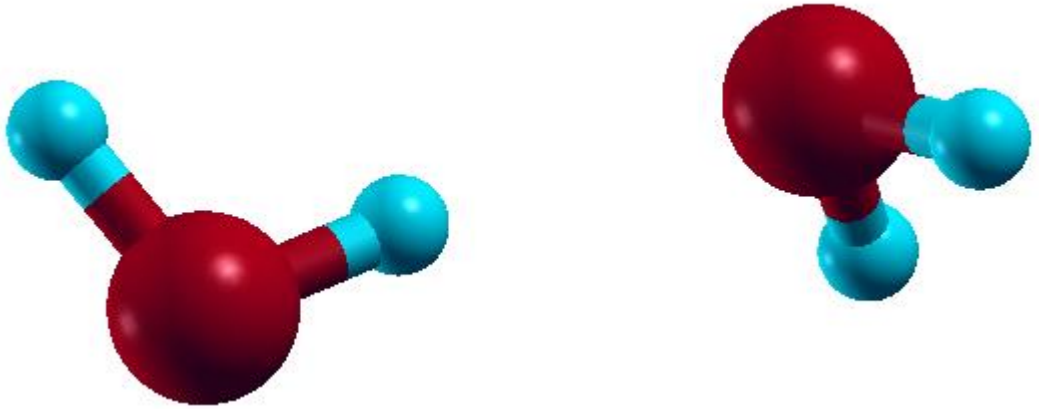

	Equilibrium O-O distance (Ang.)	Dipole moment (Debye)	Binding energy (kcal/mol)	Binding energy (couterpoise corrected) (kcal/mol)
O7.0-s2p2d1, H7.0-s2p1	2.899	2.54	5.57	5.21
O7.0-s3p3d2, H7.0-s3p2	2.897	2.45	5.48	5.48
Other calc.	2.893[a]		5.15 [a]	
Expt.	2.98[b]	2.60[b]	5.44 [b]	

https://t-ozaki.issp.u-tokyo.ac.jp/vps_pao2019/O/index.html

A series of benchmark calculations implies that BSSE is ～0.5 kcal/mol for molecular systems.

Work functions

fcc Al (111) surface

By allocating empty atoms in vacuum near the surface, one can calculate work functions accurately.

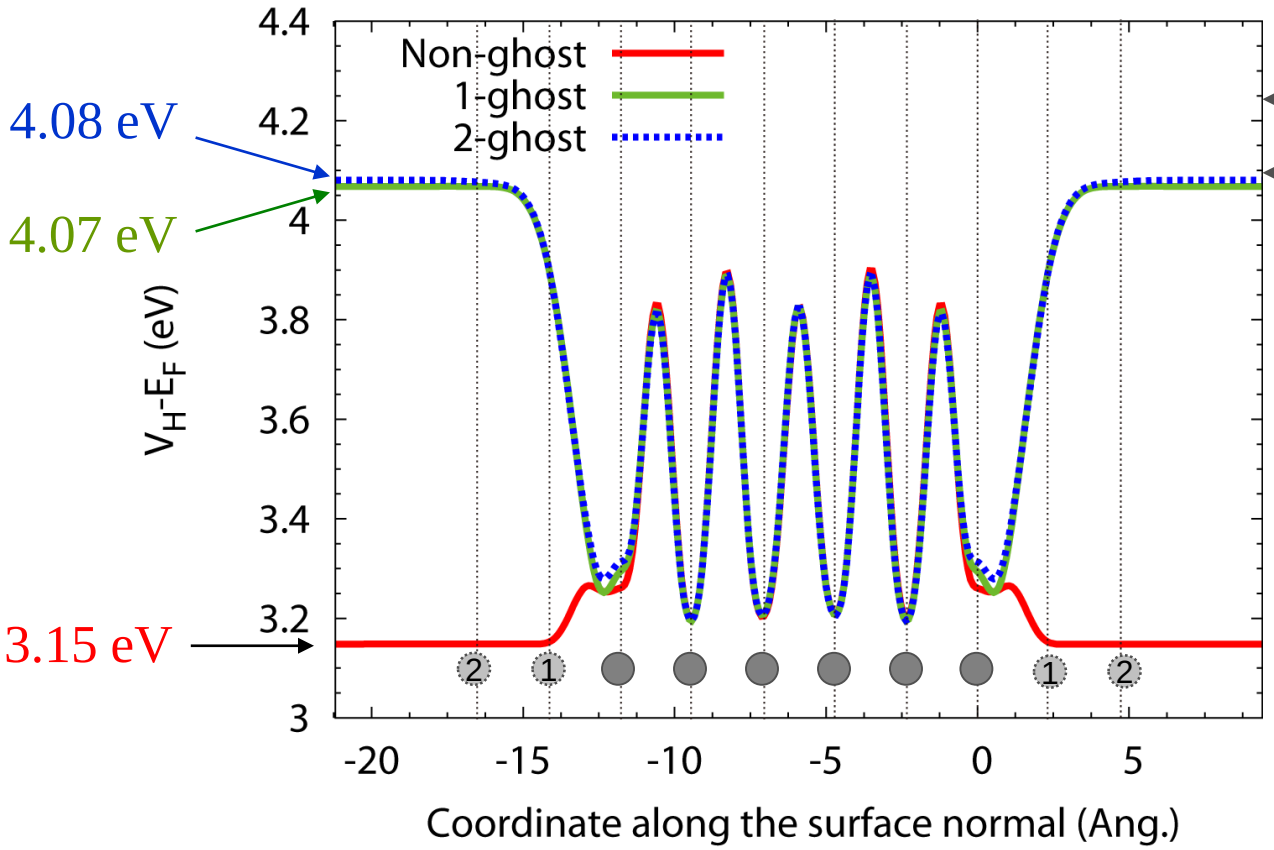

Work function

Exp : 4.24 eV

PW : 4.09 eV

Y. Morikawa *et al.*, PRB **69**, 041403(R) (2004); TABLE I.

By Jippo and Ohfuti (Fujitsu)

Al(111) fcc 1x1 6L, GGA-PBE, Fix to the equilibrium lattice parameter
Al6.0-s1p2d1, Al_PBE (Database ver. 2006)
E6.0-s1p2d1, E (Database ver. 2006)

See the page 207 in the manual.

Overcompleteness of basis functions

Total energy of fcc-Ag

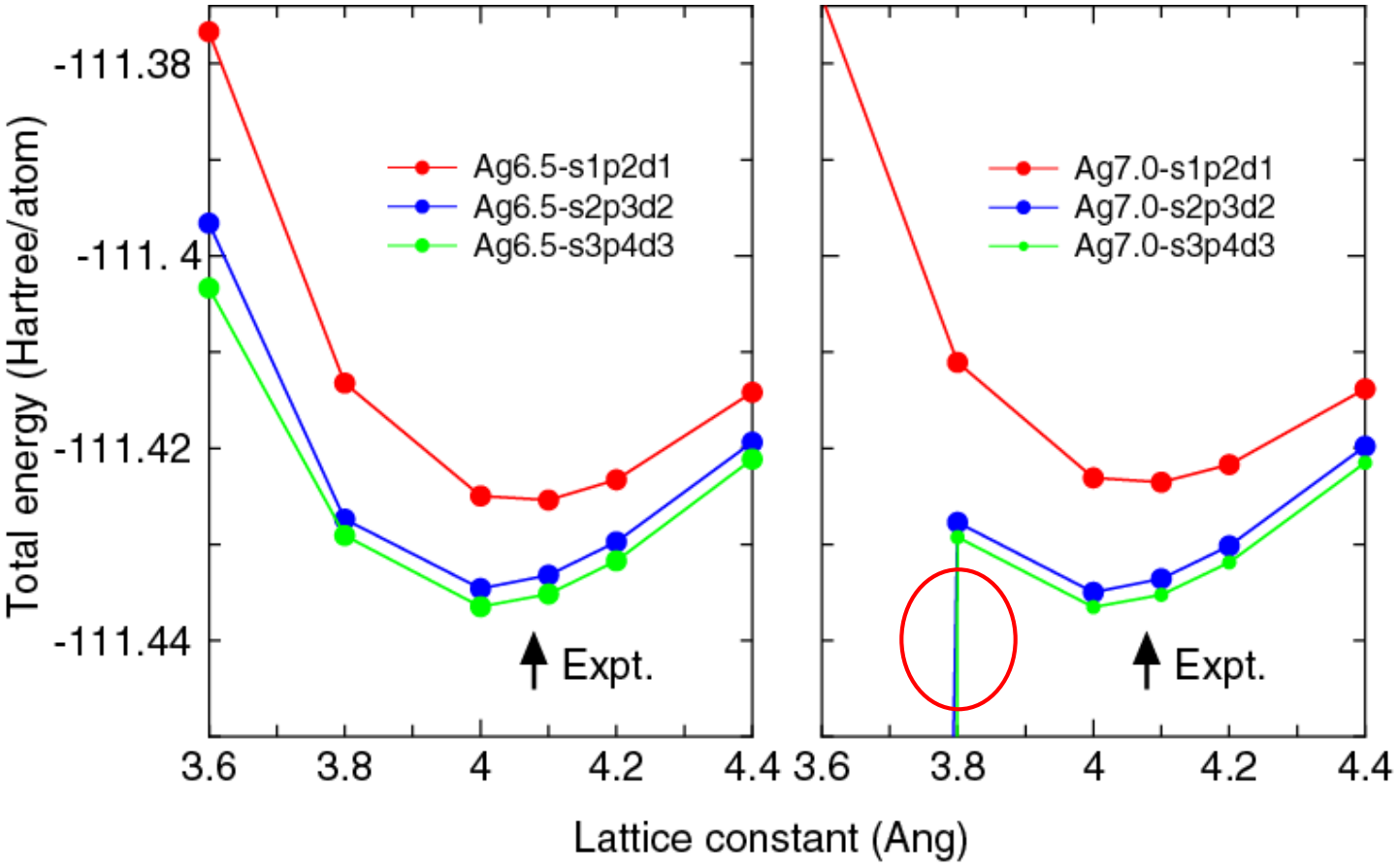

A numerical instability, called “overcompleteness”, tends to appear if a lot of basis functions are used for dense structures such as fcc, hcp, and bcc.

Cause of overcompleteness

Let's take a H_2 molecule as a simple example, and consider d→0 where d is the interatomic distance.

$$Hc = \varepsilon Sc$$

$$H = \begin{pmatrix} e & h \\ h & e \end{pmatrix}$$

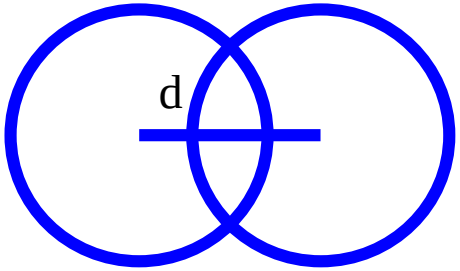

$$S = \begin{pmatrix} 1 & s \\ s & 1 \end{pmatrix}$$

$$\begin{aligned} Hc &= \varepsilon Sc \\ Hc &= \varepsilon V \lambda V^{\dagger} c \\ \lambda^{-1/2} V^{\dagger} H V \lambda^{-1/2} \lambda^{1/2} V^{\dagger} c &= \varepsilon \lambda^{1/2} V^{\dagger} c \end{aligned}$$

$$S = V \begin{pmatrix} \lambda_1 & 0 \\ 0 & \lambda_2 \end{pmatrix} V^{\dagger} = V \lambda V^{\dagger}$$

$$H' = \lambda^{-1/2} V^{\dagger} H V \lambda^{-1/2}$$

$$b = V^{\dagger} c$$

$$H' b = \varepsilon b$$

$$\lambda_1 = 1 - s \qquad v_1 = (1, -1)$$

$$\lambda_2 = 1 + s \qquad v_2 = (1, 1)$$

A round-off error arises when H' is calculated, and the error is magnified by $1/\sqrt{\lambda_1}$.

Recommendation of choices for PAO

VPS	Valence electrons	Quick	Standard	Precise
E	0.0	Kr10.0-s1p1	Kr10.0-s2p1d1	Kr10.0-s2p2d1f1
H_PBE19	1.0	H5.0-s2	H6.0-s2p1	H7.0-s2p2d1
He_PBE19	2.0	He8.0-s1p1	He8.0-s2p1	He10.0-s2p2d1
Li_PBE19	3.0	Li8.0-s3p1	Li8.0-s3p2	Li8.0-s3p2d1
Be_PBE19	2.0	Be7.0-s2p1	Be7.0-s2p2	Be7.0-s3p2d1
B_PBE19	3.0	B7.0-s2p2	B7.0-s2p2d1	B7.0-s3p2d2
C_PBE19	4.0	C6.0-s2p2	C6.0-s2p2d1	C6.0-s3p2d2
N_PBE19	5.0	N6.0-s2p2	N6.0-s2p2d1	N6.0-s3p2d2
O_PBE19	6.0	O6.0-s2p2	O6.0-s2p2d1	O6.0-s3p2d2
F_PBE19	7.0	F6.0-s2p2	F6.0-s2p2d1	F6.0-s3p3d2f1
Ne_PBE19	8.0	Ne9.0-s2p2	Ne9.0-s2p2d1	Ne9.0-s3p2d2
Na_PBE19	9.0	Na9.0-s3p2	Na9.0-s3p2d1	Na9.0-s3p2d2
Mg_PBE19	8.0	Mg9.0-s2p2	Mg9.0-s3p2d1	Mg9.0-s3p2d2
Al_PBE19	3.0	Al7.0-s2p1d1	Al7.0-s2p2d1	Al7.0-s3p2d2
Si_PBE19	4.0	Si7.0-s2p1d1	Si7.0-s2p2d1	Si7.0-s3p3d2
P_PBE19	5.0	P7.0-s2p2d1	P7.0-s2p2d1f1	P7.0-s3p2d2f1
S_PBE19	6.0	S7.0-s2p2d1	S7.0-s2p2d1f1	S7.0-s3p2d2f1
Cl_PBE19	7.0	Cl7.0-s2p2d1	Cl7.0-s2p2d1f1	Cl7.0-s3p2d2f1

See also the pages 55 and 56 in the manual.

Restarting of calculations

- After finishing your first calculation or achieving the self consistency, you may want to continue the calculation or to calculate density of states, band dispersion, molecular orbitals, and etc. using the self consistent charge in order to save the computational time. To do this, a keyword 'scf.restart' is available.

```
scf.restart          on        # on|off,default=off
```

- If the first trial for geometry optimization does not reach a convergent result or molecular a dynamics simulation is terminated due to a wall time, one can restart the geometry optimization using an input file 'System.Name.dat#' which is generated at every step for the restart calculation with the final structure.

See also the page 67 in the manual.

Output of large-sized files in binary mode

Large-scale calculations produce large-sized files in text mode such as cube files. The IO access to output such files can be very time consuming in machines of which IO access is not fast. In such a case, it is better to output those large-sized files in binary mode. The procedure is supported by the following keyword:

```
OutData.bin.flag    on    # default=off, on|off
```

Then, all large-sized files will be output in binary mode. The default is 'off'. The output binary files are converted using a small code 'bin2txt.c' stored in the directory 'source' which can be compiled as

```
gcc bin2txt.c -lm -o bin2txt
```

As a post processing, you will be able to convert as

```
./bin2txt *.bin
```

The functionality will be useful for machines of which IO access is not fast.

See also the page 320 in the manual.

Large-scale calculations

The following is a result of 'runtestL2' performed using 640 MPI processes and 1 OpenMP threads on a Xeon cluster.

$ mpirun –np 640 openmx -runtestL2 -nt 1

1	large2_example/C1000.dat	Elapsed time(s)= 777.60	diff Utot= 0.000000007341	diff Force= 0.000000008795
2	large2_example/Fe1000.dat	Elapsed time(s)= 8181.70	diff Utot= 0.000000002241	diff Force= 0.000000011061
3	large2_example/GRA1024.dat	Elapsed time(s)= 927.20	diff Utot= 0.000000012903	diff Force= 0.000000004981
4	large2_example/Ih-Ice1200.dat	Elapsed time(s)= 445.88	diff Utot= 0.000000000216	diff Force= 0.000000001451
5	large2_example/Pt500.dat	Elapsed time(s)= 2629.20	diff Utot= 0.000000015832	diff Force= 0.000000001879
6	large2_example/R-TiO2-1050.dat	Elapsed time(s)= 844.58	diff Utot= 0.000000002263	diff Force= 0.000000001108
7	large2_example/Si1000.dat	Elapsed time(s)= 658.53	diff Utot= 0.000000000404	diff Force= 0.000000000908

Total elapsed time (s) 14464.69

The elapsed time implies that geometry optimization for systems consisting of 1000 atoms is possible if several hundreds processor cores are available.

See also the page 114 in the manual.

Visualization

- Cube files such as *.tden.cube, *.sden.cube, *.dden.cube can be visualized by many software such as

  XCrySDen
  VESTA

- Also*.md file is stored in xyz format which can be visualized by XCrySDen and OpenMX Viewer.

  On phi, XCrSDen is available.

- Data on DOS and band dispersion can be visualized by gnuplot.

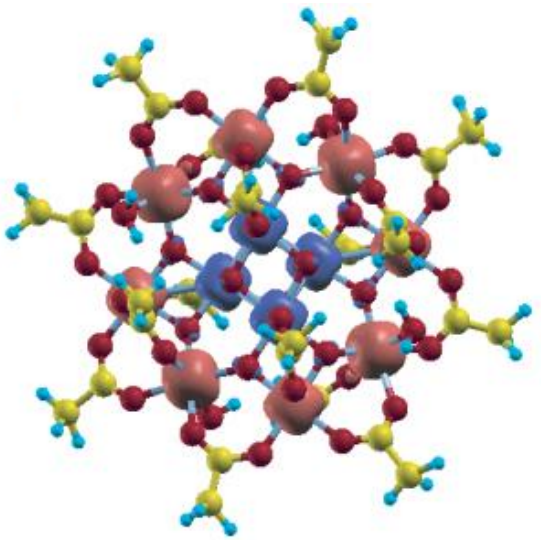

On the manual

The PDF file is available at

http://www.openmx-square.org/openmx_man3.9/openmx3.9.pdf

The manual is self-contained, the most of calculations explained in the manual are traceable by using the input file stored in the directory ‘work’.

Please try to perform those calculations one by one depending on your interests.